

**THE DESIGN AND CONSTRUCTION OF A
SMALL CYCLOTRON**

By

Mickael J. Cressman

Submitted in partial fulfillment of the requirements for the
degree of

Bachelor of Science

Houghton College

May 2006

Signature of
Author.....

Department of Physics
May 3, 2006

.....
Dr. Mark Yuly
Professor of Physics
Research Supervisor

**THE DESIGN AND
CONSTRUCTION OF A SMALL
CYCLOTRON**

By

Mickael J. Cressman

Submitted to the Department of Physics
on May 3, 2006, in partial fulfillment of the
requirement for the degree of
Bachelor of Science

Abstract

A small cyclotron is under construction at Houghton College. It utilizes a water cooled electromagnet with 15.2 cm pole faces that produces a maximum field of approximately 1.1 T with a 3.8 cm gap. The vacuum pump consists of a rotary forepump, a diffusion pump and a liquid nitrogen cold trap. The chamber consists of a brass ring with eight ports: one for evacuating the chamber, one for introducing gas, two viewports, two feedthroughs, an ion gauge, and the Faraday collector. It is sealed with two aluminum discs with Viton o-ring seals. The 'dee' electrodes are constructed from copper, with the dummy dee at ground potential and a true dee supplied with a radiofrequency signal by a function generator and an RF power amplifier. The expected energy for deuterons is 0.15 MeV, and 0.08 MeV for Helium nuclei. The immediate objective is to accelerate Helium nuclei to test the machine, and the ultimate is to accelerate deuterons to produce neutrons for inelastic scattering experiments.

Thesis Supervisor: Dr. Mark Yuly
Title: Professor of Physics

TABLE OF CONTENTS

Chapter 1 – Introduction and History of the Cyclotron.....	5
1.1 History and Description of the Cyclotron	5
1.1.1 <i>Early History and Introducti</i>	5
1.1.2 <i>The Cockcroft-Walton Generator</i>	6
1.1.3 <i>The Van de Graaf Generator</i>	7
1.1.4 <i>The Linear Accelerator</i>	8
1.1.5 <i>The Cyclotron</i>	10
1.1.6 <i>The First and Second Cyclotrons</i>	11
1.1.7 <i>The Synchrotron and Sychro-cyclotron</i>	14
1.1.8 <i>Motivation for the Houghton College Cyclotron</i>	15
1.2 History of Very Small Cyclotrons	15
1.2.1 <i>The El Cerrito Cyclotron</i>	15
1.2.2 <i>“The Cyclotrino,”</i>	16
1.2.3 <i>Fred Niell’s cyclotron</i>	16
1.2.4 <i>The Rutgers University Cyclotron</i>	17
1.2.5 <i>The Knox College Cyclotron</i>	18
Chapter 2 – Theory of the Cyclotron.....	19
2.1 Introduction	19
2.2 The Magnetic Field	20
2.3 The Electric Field	21
2.4 Focusing.....	23
2.5 Relativistic Consequences	26
Chapter 3 – Description of Apparatus.....	29
3.1 Introduction	29
3.2 The Vacuum System	29
3.3 The Cooling System	34
3.4 The Electromagnet.....	35
3.5 The Chamber	38
3.5.1 <i>The Vacuum chamber</i>	38
3.5.2 <i>The Electrodes</i>	40
3.5.3 <i>The Ion Source</i>	42
3.5.4 <i>The Faraday Collector</i>	43
3.6 The Radio Frequency Circuit	44
3.7 The Electronics	46
Chapter 4 – Conclusion.....	48
4.1 Summary	48
4.2 Future Plans	48

TABLE OF FIGURES

Figure 1. Rutherford’s gold foil experiment..	5
Figure 2. The Cockcroft Walton Generator.	6
Figure 3. Van De Graaff’s generator.	7
Figure 4. Wideröe’s linear accelerator.	9
Figure 5. The cyclotron.	10
Figure 6. The first cyclotron.	11
Figure 7. Beam current versus magnetic field strength for different oscillator voltages.	12
Figure 8. Beam current versus magnetic field strength for different hydrogen pressures	13
Figure 9. Ion trajectory and basic components of a cyclotron	19
Figure 10. Voltage versus time plot of the electric potential between the electrodes.	22
Figure 11. The focusing effects of the magnetic field	23
Figure 12. The focusing effects of the electric field.	25
Figure 13. The Houghton College Cyclotron.	29
Figure 14. The vacuum system	30
Figure 15. The vacuum pumps	49
Figure 16. The residual gas analyzer.	32
Figure 17. The RGA quadrupole filter.	33
Figure 18. Preliminary RGA results.	349
Figure 19. The cooling system.	35
Figure 20. The electromagnet.	35
Figure 21. Magnetic field vs. current.	36
Figure 22. Magnetic field vs. radius at 25 Amps.	37
Figure 23. Index for the magnet.	41
Figure 24. The vacuum chamber.	39
Figure 25. Photograph of the vacuum chamber.	40
Figure 26. The electrodes.	41
Figure 27. The electrode assembly.	41
Figure 28. The gas handling system.	42
Figure 29. The Faraday collector assembly.	43
Figure 30. The resonating circuit.	44
Figure 31. The electronics.	47
Figure 32. Cross section vs. deuteron energy for the $d(d,n)He^3$ reaction.	49

Chapter 1.

Introduction and History of the Cyclotron

1.1 History and Description of the Cyclotron

The level of understanding of the structure of matter today is due in large part to the knowledge gained from scattering experiments, where the collisions of atoms with other very small particles is studied. Several particle accelerators were developed because they could generate the fast particles needed for such experiments. While natural radiation could provide these particles, machines to accelerate particles to controllable energies and intensities were required to perform more sophisticated scattering experiments. This section will introduce the historical background of the development of these machines, especially the cyclotron.

1.1.1 Early History and Introduction

In 1911 E. Rutherford performed his famous gold foil experiment [1,2] which consisted of scattering alpha particles, emitted from naturally radioactive radium, from thin gold foil. The scattered alpha particles emitted an observable flash of light when they struck the zinc sulfide screen, as seen in Figure 1.

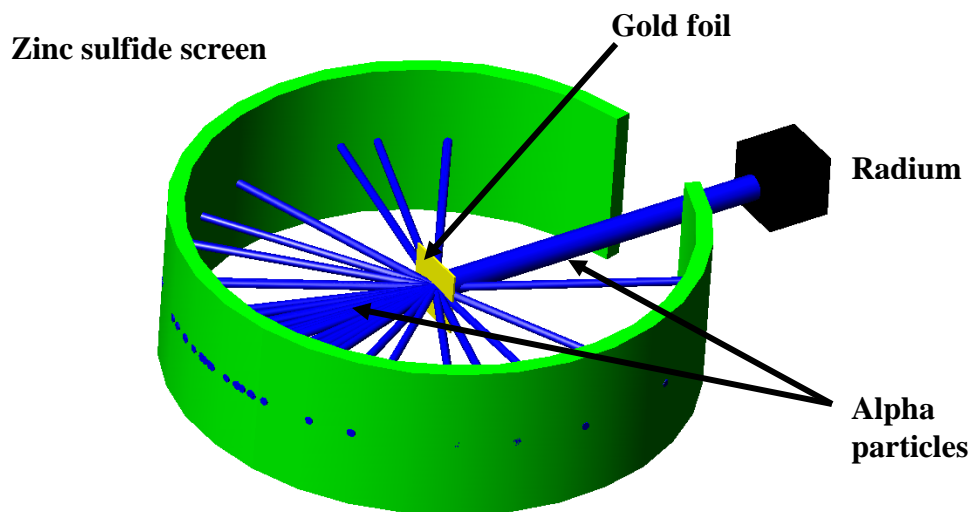


Figure 1. A schematic of Rutherford's gold foil experiment. A radium source provides the alpha particles which are allowed to strike the gold foil. The scattered alpha particles emitted an observable flash of light when they struck the zinc sulfide screen.

Rutherford found that some of the positively charged alpha particles scattered off the foil at very large angles, and did not pass through with some small deflection angle. Thus he concluded that

gold atoms are composed of small, dense, positively charged nuclei, and that most of the volume in an atom is empty space. With this discovery came the desire to artificially disintegrate the nucleus of an atom to further probe the structure of matter. The goal was to produce a controllable source of particles that were energetic enough to disintegrate light nuclei, which created a race of sorts primarily between Cockcroft and Walton, Van de Graaff, and Lawrence to create a source of energetic ions with controlled flux, direction, and energy.

1.1.2 The Cockcroft Walton Accelerator

Cockcroft and Walton worked on a single stage accelerator using very high voltages produced by a system of capacitors and switches that allowed the multiplication of voltages [3]. The idea consisted of two sets of capacitors where each capacitor in each set were in series within the set, but in parallel with the other set. The parallel connections could be changed with switches, as seen in Figure 2.

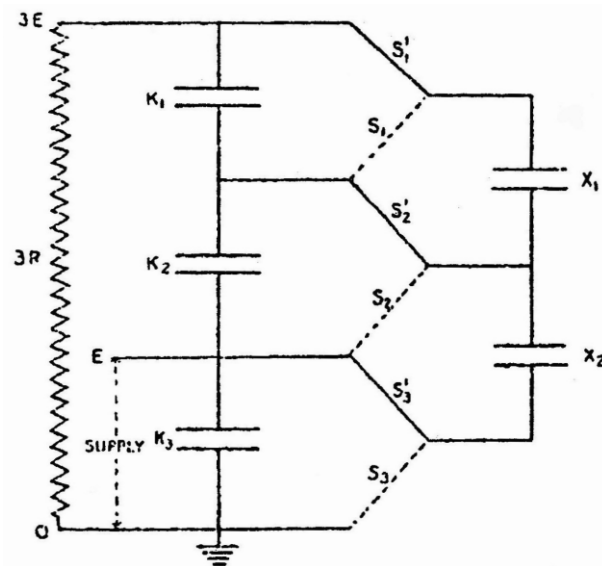


Figure 2. A schematic of the Cockcroft-Walton Generator. First, the switches S_1 through S_3 , were closed as shown by the dotted lines. Capacitors X_2 and K_3 were charged by the voltage supply, E . The switches were changed and are represented by the solid lines, so capacitors X_2 and K_2 were then charged to $E/2$. The switches were then reversed, so X_2 charged up back to E , and K_2 and X_1 shared the charge K_2 had in the last step, so each had $E/4$. This continued until the voltage across each K capacitor was E , creating a total voltage of $3E$. Diagram taken from Ref [3].

The first capacitor in one set, call it K_3 , had a voltage applied to it. A corresponding capacitor in the parallel set, X_2 , was also then charged to the same voltage, call it E . The switches were then changed, so that X_2 was in parallel with K_2 and the voltage was shared, so $E/2$ on each. The switches were

placed in their original position and X_2 was recharged to E while K_2 was in parallel with X_1 , and the voltage was shared, so $E/4$ on each. As the cycling continued the charge was pushed up the capacitor system, allowing much higher voltages than the original source.

Though the concept involved switches it is apparent that this same effect can be achieved with alternating current and diodes instead of direct current and switches. By using this idea Cockcroft and Walton produced an 800 kV potential. In a paper published in 1932 [3] Cockcroft and Walton documented the first disintegration of atomic nuclei by artificial means. Using 600 keV protons, they split a lithium nucleus into two helium nuclei. They also probed the possible disintegration of a variety of other elements, finding that 150 keV was sufficient to the task for a variety of isotopes. The maximum voltage that can be achieved by the Cockcroft Walton Generator is about 1 MV [6] as the insulation between the capacitors tends to break down at such voltages. Also, the sheer bulk of the machine itself makes it unsuitable for smaller laboratories.

1.1.3 The Van de Graaff Accelerator

Robert J. Van De Graaf took another approach to reaching very high accelerating voltages [4], of which is shown in Figure 3.

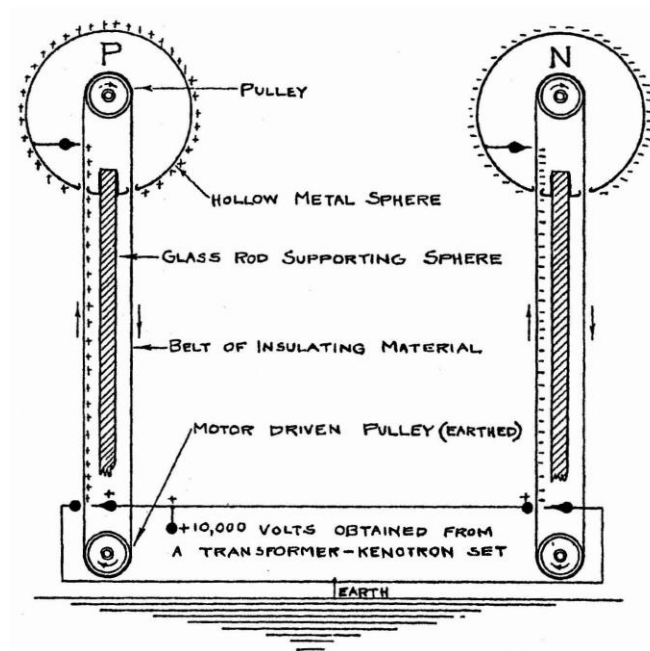


Figure 3. A schematic of Van De Graaff's generator. An insulating belt collected charge from a source at the bottom, either high voltage or triboelectric. The belt was mounted on two pulleys and was driven by an electric motor. The

charge collected at the source was transferred to the electrode at the top, which, though at a higher potential than the belt, could still gain charges because the electric field inside a conductor is always zero. Two of these devices of opposite polarity can be used to double the potential difference. Drawing taken from Ref [4].

Charge was transferred from the high voltage source to the belt either by high voltage ‘spraying’ with a metal needle brushing the belt or the triboelectric effect. In the triboelectric effect, charge transfers from one object to another through physical contact as a result of the electric properties of the materials. Materials are rated on the triboelectric series, which is a listing of materials in the order of the sign and magnitude of charge transferred when they are touched. A Van de Graaf accelerator using the triboelectric effect would then use two materials that are far apart on the series, like silk and glass to accumulate negative charge on the silk belt, or hard rubber to accumulate positive charge on the belt. The belt on two pulleys was driven by an electric motor, so it carried the charge to a hollow conductive dome called a terminal as the top pulley was mounted inside the terminal. The charge was then transferred to the terminal through another metal needle brush, as the charges were repulsed by like charges on the belt. Charge builds up on the terminal because even though it may be at a higher potential than the silk belt, the charges experience no electric field because they are inside of a conductor. Two of these devices could be used with an accelerating tube in between, one at positive potential and the other at negative to double the voltage difference. With a two terminal system, Van De Graaff achieved a potential of 1.5 MV in 1931 [5]. The limit to the potential that can be achieved by a Van De Graaff generator depend on the gas which surrounds the generator, and the radius of the terminals. Generally speaking, the maximum energy achievable with one of these generators is around 10 MV

1.1.4 The Linear Accelerator

The modern linear accelerator is a result of the work of Rolf Wideröe, published in 1928 [7]. The idea consisted of an oscillating potential to accelerate ions, whereas the Cockcroft Walton and Van De Graaff schemes used high voltages to accelerate the ions electrostatically. A tubular electrode was connected to the oscillator with other tubes at ground potential on either end of the oscillating tube, and an ion source on the far end, as seen in Figure 4.

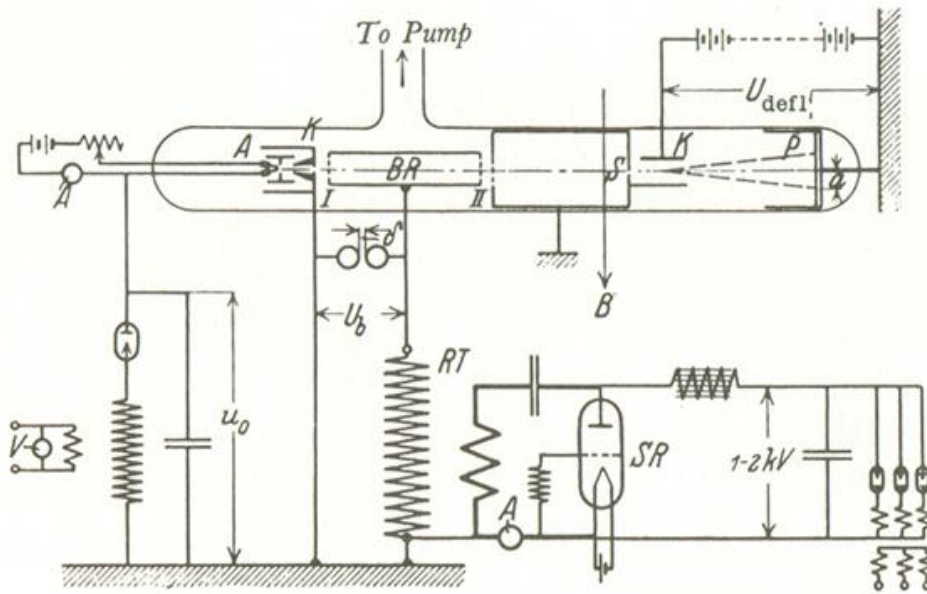


Figure 4. A schematic of Wideröe's machine. An oscillating voltage was applied to tube BR, with two other tubes A and S connected to ground on either end. An ion leaving grounded tube A was pulled towards the second tube. The voltage was timed to reverse as the ion approached the other end, and was then pushed into tube S. In this fashion the same voltage was used for the multiple acceleration of ions. Picture taken from Ref [7].

The ions traveled towards and through the first tube, A, with some initial velocity. As the ions passed between the gap between the first two tubes, A and BR, the electric field was such that the particles were pulled into tube BR. During the time spent in tube B the voltage reversed so that the ions were pushed out of BR and pulled into the third tube, S. Since there was no electric field inside tubes A and S, the voltage oscillation does not affect the particles until they approached the gap between tubes. The oscillating voltage was at a frequency specifically chosen to match the energy gain, the mass and charge of the particles, the initial velocity, and the length of the tubes. This idea can be extended to any number of tubes, though it is important to note that as the particles gain energy they travel faster. This requires each tube be longer than those that precede it, so that the time spent in each tube is the same for any given tube allowing a single frequency to be used. In this fashion the same voltage difference could be used multiple times to accelerate the charged particles, and very high voltages are not required. The design was first tested for very high ion energies by David Sloan and Ernest Lawrence [8] in 1931. The machine produced 1.26 MeV singly ionized mercury ions using electrode potentials of 42,000 V, and a machine capable of 10 MeV ions was planned.

One disadvantage of linear accelerators is that they must be constructed to accelerate a single type of particle, however, this can be an advantage as it allows higher energies by accounting for relativistic effects. As the particle gains energy, it also gains mass in accordance with relativity. To maintain resonance the ions must spend the same amount of time in each tube, so the length of the tubes must be specially tailored. This allows linear accelerators to reach much higher energies than the other accelerators yet discussed, limited by the length of the accelerator itself, and the associated cost. The beam produced by a linear accelerator is also much more highly collimated than beams produced by circular accelerators which can provide greater luminosities.

1.1.5 The Cyclotron

Ernest Orlando Lawrence first got the idea for the cyclotron from Wideröe's [9]. He took the resonance concept of Wideröe's device, and found that a uniform magnetic field could be used to bend the trajectory of the ions so that only two electrodes were needed for the multiple acceleration of ions. As seen in Figure 5, the ions were bent into a circular path orthogonal to the direction of the applied magnetic field.

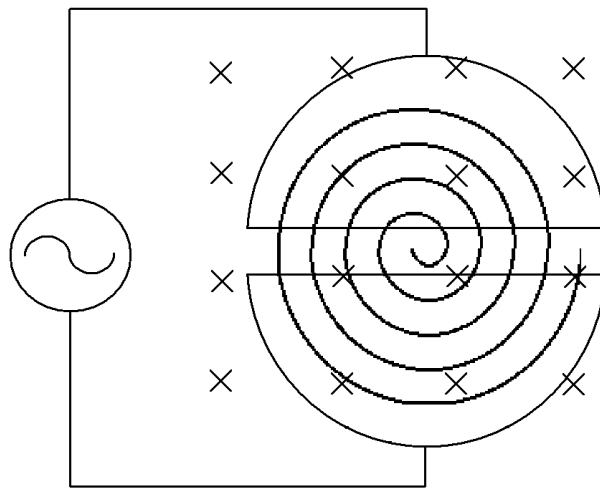


Figure 5. A basic schematic of the cyclotron. There were two electrodes, one at ground, with an oscillating potential between them. A uniform magnetic field forced the trajectory of the particles into a spiral so that the same two electrodes could be used repeatedly, circumventing the need for high voltages.

The electrodes took the shape of the letter “D,” and two of these were put face to face to form a cylindrical cavity. The uniform magnetic field permeated both, perpendicular to the plane of the electrodes. An ion source was placed at the center between the two electrodes. In the linear

accelerator, every other tube was connected to the same output of a voltage oscillator, similarly in a cyclotron, the dees (electrodes) were connected to outputs that were 180° out-of-phase. Ions generated at the source experienced an electric field between the two electrodes, and were pulled into one of them. Once inside they experienced no field because they were in a cavity in a conductor. The ions traveled in a circular path due to the magnetic field, and around to the other side of the electrode. By that time the voltage had reversed accelerated them into the second electrode. The particles traveled in a spiral path as they gained energy, and hence velocity, from the oscillating voltage. In the constant magnetic field, the oscillator frequency is constant and independent of the radius of ion trajectory. The maximum energy limit of the cyclotron is due to relativity, and is approximately 25 MeV for protons [6]. The advantage of a cyclotron to a small laboratory is it does not require high voltages and can be a highly compact device.

1.1.6 The First and Second Cyclotrons

By 1931 Milton Stanley Livingston, a graduate student working under Lawrence, completed and successfully tested the first operational cyclotron [10], shown in Figure 6.

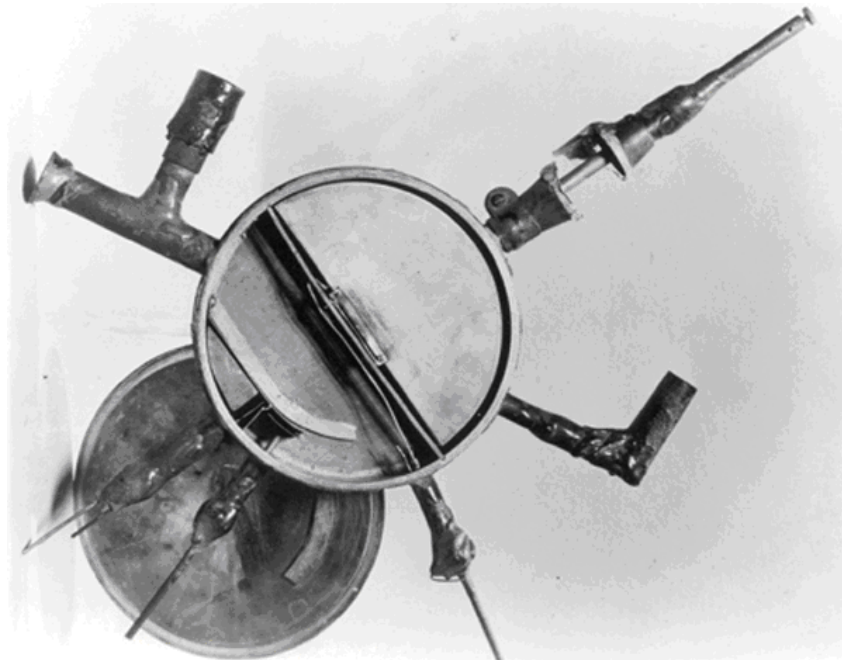


Figure 6. A photograph of the first cyclotron. Clearly visible is the dee, dummy dee, and the collector assembly. Photo taken from Ref [10].

This cyclotron utilized a 0.55 T electromagnet with pole faces 10.18 cm in diameter, and with an oscillating potential of approximately 2000 V, it produced hydrogen ions with kinetic energies of around 80 keV [6,10]. Livingston used a section of brass tube for the wall of the vacuum chamber,

with circular brass plates for the top and bottom. One of the electrodes was a full dee, and the other was a dummy dee. A dummy dee is an electrode not connected to the oscillator, and along with the vacuum chamber itself is held at ground potential. In the first cyclotron a grid was used as the dummy dee, and a grid was placed on the open face of the dee to promote uniformity in the electric field between the electrodes. It was found later that a non-uniform electric field was desirable, as will be discussed in the theory section. The electron source was a filament taken from a radio tube, and consisted of a tungsten filament running through a ceramic cylinder around which was an oxide coated nickel sheath. This system prevented the fragile filament from destructive movement under the influence of the magnetic field. Small quantities of hydrogen gas were allowed in the chamber at approximately 2×10^{-5} torr, where an amount were ionized by thermionically emitted electrons from the filament. Two 852 Radiotron tube oscillators in parallel were used to provide the oscillating voltage, and a resonating circuit to match the frequency of the ions in the magnetic field provided the power to the dee. The first cyclotron produced four peaks when collected current was plotted against the strength of the magnetic field, as seen in Figure 7.

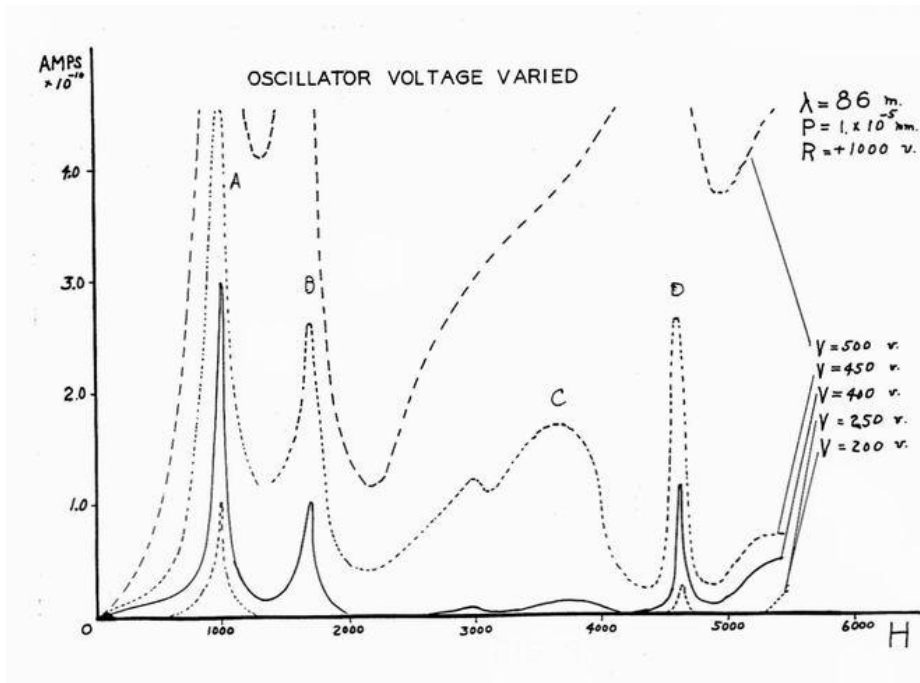


Figure 7. A plot of beam current versus magnetic field strength for different oscillator voltages. Peak A was a result of the quarter cycle effect, B was the third harmonic of resonant ions, C was caused by secondary collisions, and D was the fundamental resonance peak, and was the first evidence that the cyclotron worked. Figure taken from Ref [10].

Peak D was determined to be the resonance curve; it checked well with the predicted values, and thus was the first evidence that the cyclotron worked. Peak C was also background radiation in the chamber, and was the result of secondary collisions. It was removed by using a retarding grid set at a voltage appropriate for the oscillator voltage, by selecting a low oscillating voltage (see Figure 7), or by maintaining a relatively high hydrogen gas pressure in the chamber, as seen in Figure 8.

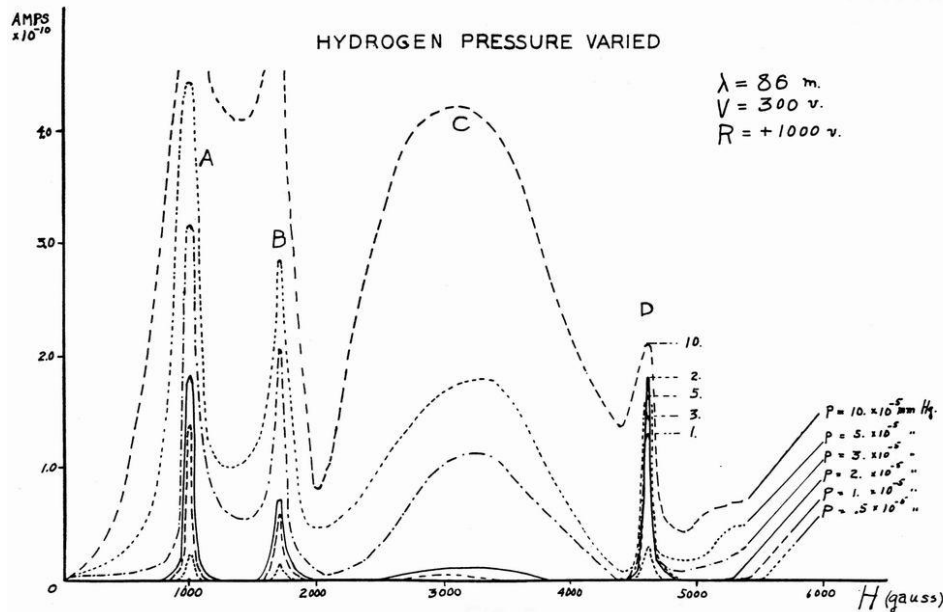


Figure 8. A plot of beam current versus magnetic field for different values of hydrogen pressure in the chamber. By lowering the Hydrogen pressure to 1×10^{-5} torr peak C was effectively eliminated. Figure taken from Ref [10].

Peak B was the third harmonic of the resonant ions in the chamber, note that it occurs at approximately $1/3$ the magnetic field of peak D. At $1/3$ the magnetic field required for fundamental resonance the ions were accelerated during the first half of one cycle, traversed a longer path in the weaker magnetic field, arrived at the electrode gap two half cycles later, and were then accelerated again to repeat the process. Though this peak was expected, it was absorbed into background radiation peak A until a collector employing a retarding potential was used. Peak A was the result of ions which had crossed the gap between electrodes once and thus been accelerated, but in the weak magnetic field the arc of trajectory was wide and carried them to the collector without further acceleration. These results proved that the magnetic resonance principle could be exploited to produce a significant current of high energy ions without the use of high voltages. Lawrence and Livingston took the next step in building a cyclotron with an electromagnet with 11 inch pole faces which accelerated protons to energies in excess of 1.2 MeV [11]. Like the first, it used a dee and

dummy dee system, constructed of brass, and situated in a brass chamber. Using this device Livingston disintegrated the atomic nucleus of lithium, reported September 15, 1932, just three months after Cockcroft and Walton did the same [12]. This second cyclotron convinced its makers that the principle of magnetic resonance was a reliable method of reaching the energies desired, and of the possibility of achieving its relativistic upper theoretical limit. As a particle is accelerated it gains energy, and in accordance with the special theory of relativity it also gains mass. This extra mass causes the ions to travel larger orbits in the magnetic field than they otherwise would at the same speed, and thus fall out of resonance with the oscillator. This causes the cyclotron to cease to function at 25 MeV for protons [6]. The problem was first predicted by Hans Bethe and M. E. Rose [13], and was solved with the advent of the synchrocyclotron.

1.1.7 The Synchrotron and Synchro-cyclotron

The synchrocyclotron operates under the same principle as the cyclotron, however it does not operate at a fixed frequency. Instead a packet of ions is chosen to be accelerated, and the frequency of the oscillating electric field is modulated as they gain mass in accordance with relativity. The pulsed beam of ions is used at the end of each frequency ramp, and the process begins again with a new packet of ions. The advantage of the synchrocyclotron is that it can achieve higher energies than a similarly sized cyclotron by overcoming the limit imposed by relativity, without a great difference in design or increase in expense. For small laboratories desiring particles with energies lower than 25 Mev, the cyclotron is better suited, as frequency synching is not required.

The synchrotron also uses a modulated electric field frequency to accelerate relativistic ions, but it also uses a ramped magnetic field to adjust the path of the particles as they gain mass. Synchrotrons are best for very high energy particle collisions as they are the only extant accelerators than can reach very high energies, as they are limited only by the size and power of the device. The most notable synchrotron is the Large Hadron Collider [14] being constructed in CERN, and due for completion in the year 2007. This massive accelerator will collide two beams of protons, each at 7 TeV.

Synchrocyclotrons and synchrotrons have one other significant distinction from the cyclotron and that is the pulsed nature of the machines. The frequency ramping of the two newer machines dictates accelerating packets of ions as opposed to a continuous beam which means that while a cyclotron has a lower energy range, it also produces a higher beam current.

1.1.8 Motivation of the Houghton College Cyclotron

The purpose of the Houghton College cyclotron project is to create an artificial neutron source which could then be used to collect cross section data for various inelastic neutron scattering experiments. The neutrons will be produced with the cyclotron by accelerating deuterons into a copper target, thereby impregnating it with deuterons. As deuterons continue to collide with the copper target, some will interact with the embedded deuterons in the $d(d,n)^3\text{He}$ and $d(d,p)^3\text{H}$ reactions. If the former occurs, the outgoing neutrons will be produced with 2.8 MeV. The electrically neutral neutrons will pass through the chamber walls and can then be used for inelastic scattering measurements.

1.2 History of Very Small Cyclotrons

From the very start, each generation of cyclotrons was built to be larger and achieve higher energies than those that preceded it. A limited number of very small cyclotrons have been reported, and this section will briefly introduce them.

1.2.1 The El Cerrito Cyclotron

The El Cerrito cyclotron [15,16] was built at the El Cerrito High School by high school students in 1947. Approximately 8 kilometers of 13 gauge copper wire were wound around the six inch pole pieces for the electromagnet. The first attempted vacuum chamber was made of curved sheets of copper that clamped around the magnet's poles. Using gaskets to seal the chamber, the machine produced a beam current of 1.5 microamperes. However, the system could not maintain vacuum and a new design was sought. The modified chamber consisted of a section of 16.5 cm brass tubing used as the wall of the chamber, and two 0.3 cm thick circular steel plates as the top and bottom. The bottom plate was soldered to the brass, the top plate was screwed to the bottom plate with a rubber gasket between the brass and steel to form a seal. The El Cerrito Cyclotron used only one dee, and did not employ a 'dummy dee,' but rather held the chamber itself at ground. The vacuum system had two stages, using a mechanical roughing pump and a mercury diffusion pump, and the vacuum was monitored by a MacLeod gauge and a Pirani gauge. The oscillator was a single 304TH tube with direct feedback, and the amplifier used two 872A mercury vapor tubes. The system was operated at 1,600 watts and could provide a maximum of 2,000 watts to the electrodes. The team accelerated protons by ionizing hydrogen gas with a hot filament, and with the new vacuum chamber a beam of 7 microamperes was produced.

1.2.2 *The “Cyclotrino”*

The Cyclotrino [17] was built at the Lawrence Berkeley Laboratory at the University of California in 1987 for the purpose of making accelerator mass spectrometry measurements (AMS), while minimizing cost, size, and complexity of operation. AMS is a method of measuring the ratio of mass to charge of particles by determining the deflection of trajectory in a magnetic field. The magnet used was a 30.5 cm Varian NMR type electromagnet, which consumed 500 watts during operation at approximately 1 T. A dee and dummy dee system was used with the electrodes separated by approximately 1 mm. The dummy dee consisted of two pieces to allow a port for the cesium beam to enter the chamber, which spiraled in the magnet field and struck a carbon target. This produced the carbon ions that were then accelerated spectrometry measurements. The RF was provided by a ham radio transceiver, using an oven controlled crystal. The vacuum was produced by a vacuum reservoir with a cryopump system. It is interesting to note that although a permanent magnet was considered for the Cyclotrino, it used an electromagnet because the field could be tuned which was convenient for the development of the machine.

1.2.3 *Fred Niell’s Cyclotron*

Fred Niell built a small functioning cyclotron [18] during his senior year of high school, 1994 and 1995. The magnet yoke was soft iron scrap, and the pole pieces were 11.4 cm steel round stock which were then wound with 13.5 gauge wire. The vacuum chamber was 5.7 cm section of 15.2 cm stainless steel pipe with 0.6 cm thick walls. The faces of the chamber were annealed glass plates, with the external air pressure used to clamp them to the stainless steel ring, with vacuum grease to ensure a seal. A system of two brass dees with differing radii allowed for ion extraction. The dees were held in place with bent glass rods, which also raised both dees off the bottom plate. To accelerate metal ions, either a filament was created from that metal, or a nichrome wire was coated with the metal, and raised to a negative potential. For a collector, a small copper sheet was set into the path of ions leaving the larger dee, which drew electrons to itself when the ion beam was incident. The RF was supplied by a surplus generator, and a push-pull amplifier using triode vacuum tubes. A mechanical roughing pump with a cold trap were used to evacuate the chamber, and a thermocouple and ion gauge monitored the vacuum.

1.2.4 *The Rutgers University Cyclotron*

The physics department of Rutgers University of New Jersey has built two cyclotrons [19,20], one a 22.9 cm diameter prototype and the other was the final 30.5 cm diameter machine, finished in 2001. The prototype operated at 0.889 T, using a dee and dummy dee design. The prototype chamber was constructed for use in the 30.5 cm cyclotron that was the ultimate goal of this project, and so was much larger than required. It was stainless steel, as were the ports and flanges. The top and bottom plates were 0.6 cm aluminum, sealed with Viton O-rings. The chamber itself was 27.9 cm inside diameter, and the assembly was supported by a 1.3 cm thick copper rod that also connected the dee to the RF matching transformer. The filament was mounted on the dummy dee, and was powered by wires that entered and exited through two diametrically placed feed-throughs. The filament was kept isolated from ground so it could be negatively biased to increase the energy of the emitted electrons. The oscillator used an HP8165 digital programmable RF signal source, which offered an easy method of tuning the frequency. An ENI350L 100 watt solid state amplifier provided the RF power to accelerate the protons. The beam was measured with a Faraday collector, constructed of a 0.9 cm diameter short brass rod shielded by copper tubing which was cut to reveal the brass rod on only one side. This opening faced the positive ion beam to allow for a more accurate reading. The copper tube also shielded the collector from the RF signal. A phosphorescent screen could be inserted into the chamber in order to determine the vertical position of the beam.

The larger machine used a 30.5 cm pole face electromagnet that operated in excess of 1.0 T, with the same chamber as the 22.9 cm cyclotron but with a different ion source. The negatively biased filament was mounted in a block of ceramic material to which hydrogen gas was supplied through a small hole. The ion source was then covered with a ceramic plate with an aperture, and mounted near the chamber floor. This design allowed a cone of protons to stream out in the center of the evacuated cyclotron chamber, while maintaining a higher pressure of hydrogen around the filament. The RF signal was produced using a HP8656B signal source, which had greater frequency resolution than the HP8165, and an ENI NMR-300L solid state amplifier. Its maximum output was 2,500 W, but was usually operated at 50 W with satisfactory results. The vacuum system of both machines used a mechanical fore pump, a diffusion pump and an LN₂ cold trap.

1.2.5 *The Knox College Cyclotron*

A small cyclotron was constructed at Knox College as part of the honors project of Jeff Smith during the academic year of 2000-2001 [21]. The magnet was a nuclear magnetic resonance magnet with a maximum field of 2 T and approximately 20 cm diameter pole faces. Two dees were constructed of copper and were mounted with blocks of insulating dielectric material such that they could be moved independently of each other. The chamber itself was constructed of 0.48 cm thick brass. The ion source was a coiled coated tungsten filament mounted in the center of the chamber, the emitted electrons ionizing the low pressure hydrogen gas in the chamber. As the ion source was considered experimental and a weak design aspect, it was made to be completely removable. An extractor system was designed with a negatively charged deflection plate, but the cyclotron also had a Faraday collector that was a small metal plate that could be inserted into the beam. The dees were operated at 3,750 V, using a manually adjustable resonating circuit. The capacitance of the dee's was not measured before building the resonating circuit, rather trial and error was used to tune the circuit. A large 15.2 cm diameter diffusion pump was used to create the vacuum. The electrical feed-throughs were made from nylon plugs, o-rings, and brass screws and were held in place with Plumber's Goop[™]. For the gas and Faraday collector, rubber stoppers with a hole drilled along their axes of symmetry provided the seal. Also, like Niell, the external air pressure was used to seal the top plate to the rest of the chamber. The cyclotron was not successfully tested by the publication of Ref [20], the problem being that the magnetic field caused the wires that powered the ion source to move and short the dees.

Chapter 2.
Theory of the Cyclotron

2.1 Introduction

The theory of operation of the cyclotron shall be discussed in this section, considering the magnetic electric fields, focusing, and the consequences of relativity for the cyclotron.

The use of a magnetic field in a cyclotron is what differentiates the cyclotron from the linear particle accelerators that preceded it, and is what allows for the acceleration of light ions to high velocities without using high voltages. Cyclotrons are not always the most practical accelerators for heavy ions, as the mass of the particles would make the radius of orbit prohibitively large, as will be seen. In the cyclotron there are two hollow semicircular plate electrodes, called “dees” because they are shaped like the capital letter “D,” as seen in Figure 9.

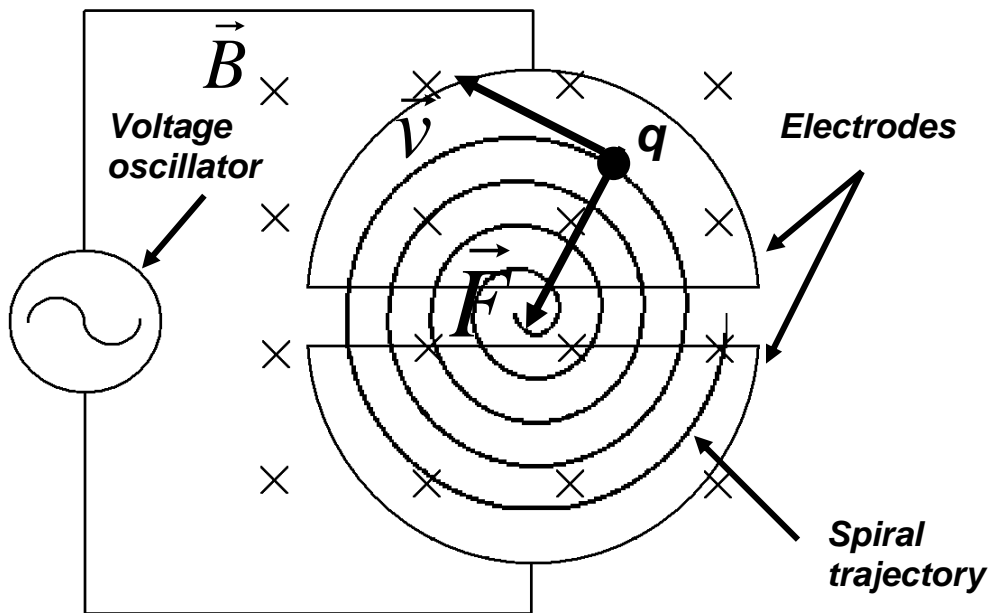


Figure 9. A schematic showing the shape and arrangement of the electrodes, the orientation of the magnetic field (into the plane of the paper), and the velocity and spiral path of a positively charged ion. The force due to the magnetic field on the ions is directed towards the center of the orbit.

The ions travel in the region of space inside the electrodes and in the gap between them. The centrally located filament emits electrons which ionize the low pressure gas in the vacuum chamber, producing

a source of ions between the two dees. An oscillating electric field between these electrodes is the source of energy for the acceleration of the ions; every time an ion crosses the gap between the dees the electric field gives the ion a ‘kick.’ Permeating the chamber and perpendicular to the path of the ion is a magnetic field, as seen in Figure 6, which causes the ions to move along a circular path.

2.2 The Magnetic Field

This magnetic field provides the Lorentz force on the ions, which is equivalent to

$$\vec{F} = q\vec{v} \times \vec{B}, \quad (1)$$

where \vec{F} is the force, q is the charge of the ion, \vec{v} is the velocity of the ion, and \vec{B} is the magnetic field. Because the direction of the force is the cross product between the velocity of the particle and the magnetic field, the Lorentz force is perpendicular to both. The largest component of the velocity of the ion is in the plane perpendicular to the magnetic field, because of the accelerating electric field and the focusing effects of the electric and magnetic fields, discussed later. Because of the field the force on the ion is centrally directed, causing the ion to follow a circular path. The spiral path shown in Figure 6 is a result of the acceleration of the ion due to the oscillating electric field. Since the accelerated ions travel in a plane normal to the magnetic field, the magnitude of the Lorentz force is

$$F = qvB. \quad (2)$$

This then is the non-relativistic centripetal force on the ion, and if m is the mass of the ion and r is the radius of the orbit,

$$\frac{mv^2}{r} = qvB. \quad (3)$$

The frequency of revolution is the speed of the particle divided by the distance of one complete revolution, or

$$f = \frac{v}{2\pi r}. \quad (4)$$

Solving (3) for v and substituting into (4) gives:

$$f = \frac{qB}{2\pi m}. \quad (5)$$

The frequency of revolution is independent of the velocity of the particle, v , and the radius, r . This is what makes it possible to apply a constant frequency voltage oscillation to the electrodes: as the ion is accelerated, its radius of orbit will increase, however, the extra distance the ion must travel in its orbit is exactly counteracted by the increased speed of the particle, and so it will approach the gap between the electrodes at constant intervals. It should be noted that this resonance breaks down as the ions approach relativistic velocities, due to relativistic mass change. This is important because for sub-relativistic velocities the frequency of the electric field applied to the dees can be constant, and the same ions will get the same ‘kick’ on every half revolution.

Finally, using (3), the non-relativistic kinetic energy of the ions can be given in terms of the radius of the final orbit, R .

$$T = \frac{1}{2}mv^2 = \frac{q^2 B^2 R^2}{2m}. \quad (6)$$

Note that final kinetic energy depends only on the squares of final radius of orbit and the applied magnetic field. Thus, the maximum energy can be increased dramatically by making the chamber larger, or by applying a stronger magnetic field.

2.3 The Electric Field

The oscillating electric field supplies the energy to accelerate the particles to high velocities. As the ions travel in a circular path in a magnetic field, they will cross the gap between electrodes twice in a revolution, each time receiving a ‘kick.’ Thus the electric field must oscillate at the natural frequency of the ions under consideration in the given magnetic field. However, the ions are continually produced from electrons ejected from the filament and will have some initial random velocity, so each particle will be accelerated during a different part of the RF cycle, thereby experiencing a different voltage level. The electrons emitted from the filament are quickly removed, for being extremely light particles their orbit radius is very small and they travel in helical paths and collide with the lid of the chamber. Figure 10 shows a voltage versus time plot of the potential difference between the

electrodes. Ions that are entirely in phase with the RF signal cross the gap at time 2, and so receive the maximum amount of energy at each crossing. Ions crossing at times 1 or 3, however, are out of phase with the cyclotron's frequency and so experience only a fraction of the maximum possible energy gain.

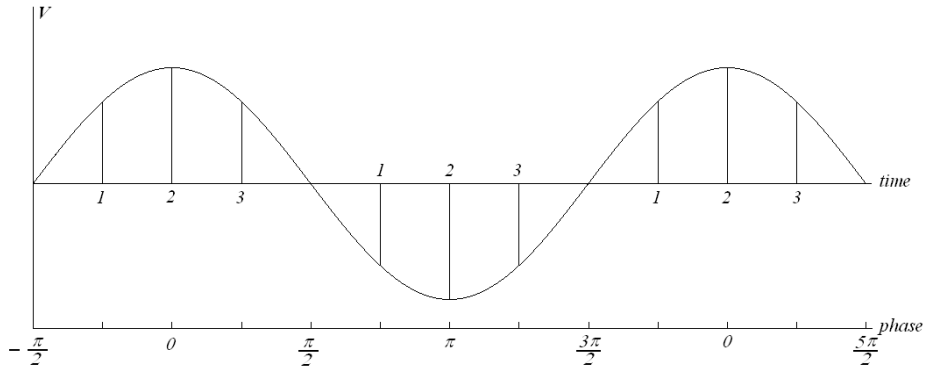


Figure 10. A voltage versus time plot of the electric potential between the electrodes. Ions crossing the gap at time 2 are in phase with the RF signal, and receive the maximum amount of energy at each crossing.

Here again the unique design of the cyclotron accounts for a major difference between it and linear accelerators. In linear accelerators faster than average ions cross the potential difference early, at a time analogous to time 1 in Figure 7, therefore they receive less energy than their fellows and slow down relative to the average speed of the particles. Thus, particles in linear accelerators are slowly pushed into the same phase, resulting in a pulsed beam. This is known as phase stability. In cyclotrons, however, particles that are somewhat out of phase stay out of phase, and there is no phase stability. However, the maximum energy is the same for each particle since the non-relativistic kinetic energy is given by the number of accelerations the particle experiences, N , times the average energy it gains from each acceleration, Vq , where V is the average voltage across the electrodes for each acceleration and q is the charge of the ion.

$$T = NVq. \quad (7)$$

Thus particles that are out of phase with the maximum voltage merely require more orbits to reach the maximum velocity.

2.4 Focusing

Thus far in this chapter only the idealized form of the cyclotron has been discussed, a cyclotron with particles that travel exactly on the median plane, with a constant magnetic field throughout the chamber, with a constant electric field between the electrodes at any given moment in time, and with ions that do not interact with each other. Of course in the laboratory this is not the case, which has important and useful ramifications. As the ions in the cyclotron are formed by ionizing a gas already in the chamber, they will have some small initial velocity, which will almost certainly not be in the median plane. Even a small velocity component out of the median plane would, after the course of several revolutions, force the ion well out of the median plane as it follows a helical trajectory, ending in a collision with an electrode or the vacuum chamber walls. Hence, the beam produced by the cyclotron would be limited to those ions with no out of plane velocity component. Fortunately, there are focusing effects due to the non-constant electric and magnetic fields that mitigate this problem.

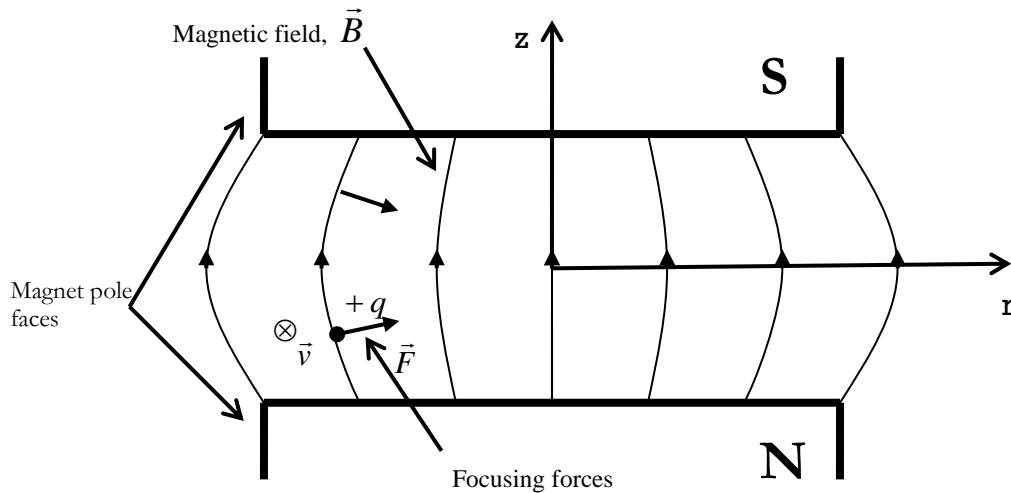


Figure 11. A schematic of the focusing effects of the magnetic field. The field ‘fringes’ at the edge of the magnet pole faces which provides a focusing force, shown in the figure on a positive ion moving into the plane of the paper below the median plane, and the force which adjusts its trajectory.

Magnetic fields are not typically uniform. In the case of electromagnets used for cyclotrons, the field tends to be strongest at the center of the pole faces and diminishes towards the edge. This results in a magnetic field where the field lines are straighter in the center and more bowed out towards the periphery. This is known as fringing and is responsible for the magnetic focusing of ions in a

cyclotron. The Lorentz force the ions experience due to the non-uniform magnetic field pushes them back towards the median plane, as in Figure 11. A useful way to parameterize the decrease of the vertical magnetic field component is:

$$B_z = B_{z_0} \left(\frac{r_0}{r} \right)^n, \quad (8)$$

where B_z is the vertical component of the magnetic field at some radius r , B_{z_0} is the vertical component of the magnetic field at some radius r_0 , and n is known as the index and is a positive constant. The index describes the radial dependence of the vertical magnetic field, so lets solve for it. Begin by taking the logarithm of both sides, yielding

$$\ln B_z - \ln B_{z_0} = n \ln r_0 - n \ln r. \quad (9)$$

After differentiating, this expression becomes

$$\frac{1}{B_z} \frac{dB_z}{dr} = -n \frac{1}{r}, \quad (10)$$

and n can be written as

$$n = -\frac{r}{B_z} \frac{dB_z}{dr}. \quad (11)$$

It has been shown that the best radial dependence of the vertical magnetic field is n increasing approximately linearly with the radius from zero at the center [4]. With this shape the frequency of revolution remains nearly constant while still providing enough focusing force. The amount of desirable focusing force depends on the number of revolutions of the particle, because as the magnetic field decreases the angular frequency decreases and the particles will drop out of resonance. Thus for large accelerators a small decrease is desirable, to maintain resonance, and for smaller machines a larger increase index is more appropriate, to provide stronger focusing.

The farther the ion is from the median plane, the stronger the focusing force it experiences. It is also important to note that the magnetic focusing force is linearly proportional to the tangential component

of the velocity, so this focusing mechanism is effective even at high energies. Magnetic field focusing is most important near the maximum energy limit of the ions because the closer to the energy limit the ions are, the farther they are from the center of the magnet, and the fringe field provides a stronger focusing force.

The oscillating electric field is also useful for focusing the ions on the median plane, which is accomplished by the same fringing effect, as seen in figure 12.

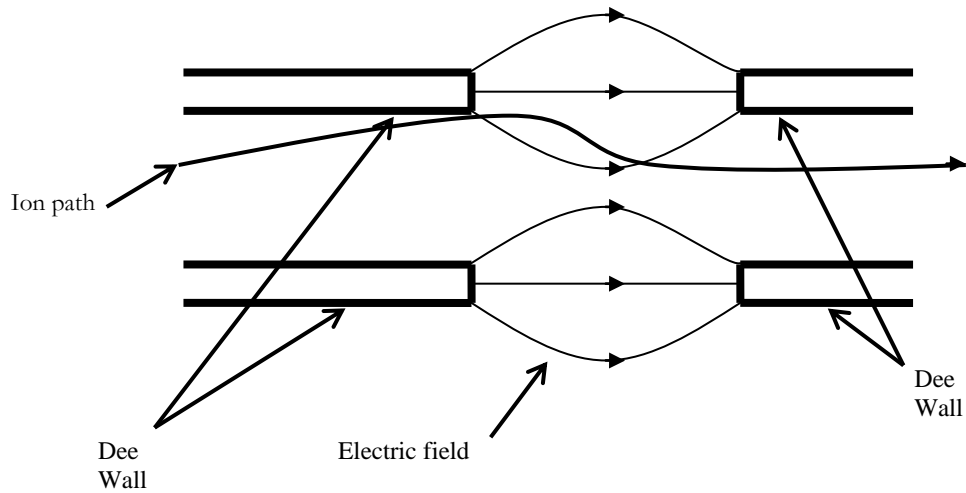


Figure 12. A schematic of the focusing effects of the electric field. A positive ion traveling through the gap out of the median plane will enter the fringe field, which will force the particle towards the median plane. As the ion exits the fringe field it is moving faster than when it entered, so the fringing of the electric field will affect the particle for a shorter time, resulting in a focusing of the ion trajectory.

If any ions are not in the median plane they are directed toward it by the initial electric field between the dees, known as the convergent field. As the ions exit the field, through what it known as the divergent field, they are deflected back out of the median plane. However, the ions are accelerated in the electric field, and so are moving with greater speed when exiting the field than when entering and spend less time in the divergent field. Thus, the net effect of the vertical component of the electric field is to direct wayward ions back to the median plane.

Another electric field focusing mechanism acting in a cyclotron also depends on the vertical component of the electric field. Since the electric field is changing, there are a number of accelerated

ions that enter the gap between dees when there is a stronger electric field than when they exit the gap. The result of this is an effectively stronger convergent field than divergent field, and the ions are focused. The opposite is also true, however, for ions entering the gap when the electric field is weaker than when they exit, and these ions are pushed away from the median plane, which results in a smaller, tighter beam. In both cases of electric focusing, the time spent in the lens decreases the faster the ions travel, thus it is only effective at relatively low velocities.

It is interesting to note that in the second cyclotron built [9], the electrode was 1 cm thick, and the ion beam produced was less than one mm wide, due to the focusing of the electric and magnetic fields

2.5 Relativistic Consequences

As one might expect, cyclotrons are subject to limits imposed by the special theory of relativity. As an object acquires energy its mass increases in accordance with the mass energy equivalence relation. Recall from (5) that the frequency of revolution depends on the mass of the accelerated ion. The relativistic mass is

$$m = \frac{m_o}{\sqrt{1 - \frac{v^2}{c^2}}}, \quad (12)$$

where m_o is the rest mass of the ion, v is the velocity of the ion, and c is the speed of light in a vacuum. (5) then becomes

$$f_{rel} = \frac{qB}{2\pi m_o} \sqrt{1 - \frac{v^2}{c^2}}. \quad (13)$$

So, as the ions are accelerated their natural frequency of revolution in the magnetic field decreases, and the ions lose resonance. The resulting phase shift becomes greater the more revolutions the ions make, so this problem can be somewhat circumvented by using higher voltages on the electrodes allowing the ions to reach comparable energies with fewer revolutions. Of course, though any phase shift will reduce the efficiency of the machine, it is not until the shift reaches $\pi/2$ radians that the machine begins to work against itself. To determine the limit on maximum energy due to relativistic effects of a cyclotron, compute the phase difference:

$$\Delta\Phi = 2\pi ft - 2\pi f_{rel}t = \frac{\pi}{2}, \quad (14)$$

where f is the frequency of the RF signal, f_{rel} is the relativistic frequency of the particle's orbit, and t is time. Using (5) and (13) this becomes

$$\frac{qB}{2\pi m_o} \left(1 - \sqrt{1 - \frac{v^2}{c^2}} \right) = \frac{1}{4t}. \quad (15)$$

Also, the kinetic energy of each particle will be the energy gained every revolution, $2Vq$, times the number of revolutions, ft . Mathematically this is written

$$T = 2Vqft, \quad (16)$$

where T is the kinetic energy of a particle and V is the voltage difference across the electrodes when the ions pass through the gap. The factor of 2 is present because an ion is accelerated twice on every orbit. Setting this equal to the relativistic definition of kinetic energy yields

$$2Vqft = \frac{1}{\sqrt{1 - \frac{v^2}{c^2}}} m_o c^2 - m_o c^2. \quad (17)$$

Using (13) and solving for t , the time required to accelerate an ion to velocity v :

$$t = \frac{m_o^2 c^2 \pi}{VBq^2} \left[\frac{1}{1 - \frac{v^2}{c^2}} - \frac{1}{\sqrt{1 - \frac{v^2}{c^2}}} \right], \quad (18)$$

which can then be substituted into (15)

$$\frac{2m_0c^2}{Vq} \left[\frac{1}{1 - \frac{v^2}{c^2}} - \frac{1}{\sqrt{1 - \frac{v^2}{c^2}}} \right] = \frac{1}{1 - \sqrt{1 - \frac{v^2}{c^2}}}. \quad (19)$$

This expression can then be solved numerically for the velocity, which in turns gives the energy. For a deuteron in an accelerating potential of 1,000 volts, the energy limit is 1.94 MeV, for an accelerating potential of 10,000 volts, the limit is 6.13 MeV, and for an accelerating potential of 20,000 volts, the limit is 8.67 MeV. Since the expected energy of the Houghton College Cyclotron is 150 keV for deuterons and 309 keV for Helium nuclei, relativity will not be a limiting factor.

It is important to note that the effects of relativity can be countered by more than just increasing the electrode voltage, it can also be mitigated by adjusting the shape and strength of the magnetic field. The actual relativistic limit for magnetic resonators accelerating protons is closer to 25 MeV. To achieve the maximum energy of the ions, the magnetic field must be chosen that best represents the balance of focusing and resonance, a complicated issue. For a more in-depth discussion please see Ref. [22].

Chapter 3.

Description of the Cyclotron

3.1 Introduction

The main components of the Houghton College Cyclotron are the vacuum system, the cooling system, the electromagnet, the ion source and gas handling system, the vacuum chamber, the RF circuit, and the remote control system. The apparatus itself is in a concrete brick room with an interlock control system to prevent the accelerator from being turned on when a person is in the room. The cyclotron can be seen in Figure 13, including the magnet, vacuum system, and electronics rack.

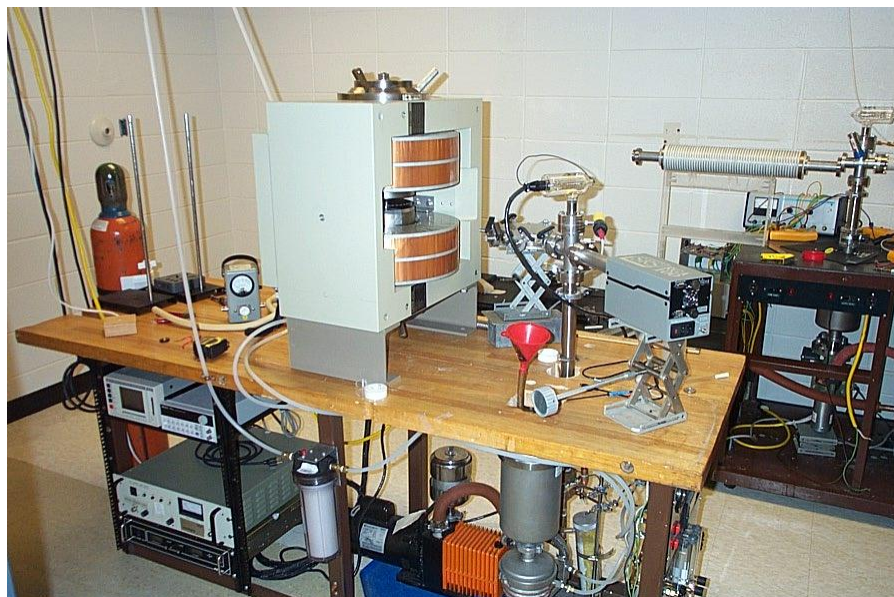


Figure 13. A photograph of the cyclotron. Clearly visible are the vacuum pumps underneath the table and to the right, the electronics rack to the left, the gas cylinder to the far left, the vacuum gauges to the right of the magnet, and the magnet.

3.2 The Vacuum System

The vacuum system, shown in Figure 14, consists of a foreline of copper pipe with soldered joints, and the rest of the system which uses stainless steel nipples, tees, and elbows. Air is removed from the chamber by a CIT-ALCATEL 2012A rotary fore-pump, an Innovac R220 diffusion pump, and a Kurt J. Lesker TNR6XA150QF cold trap, all shown in Figure 15. The fore-pump is used to rough the

vacuum down to approximately 10^{-3} torr, then the diffusion pump is engaged. Also at this time liquid nitrogen is added to the cold trap. When the pressure reaches approximately 5×10^{-6} torr the gas is added to the system using a needle valve until the pressure rises to approximately 5×10^{-5} torr. At this level at least 90% of the gas in the chamber has been purposefully introduced, and the pressure will still be low enough to allow many ions to be fully accelerated without collisions with gas molecules. This is found by calculating the mean free path of a particle in the rarefied gas. If the mean free path is longer than the trajectory of an ion that has completed a full acceleration cycle, then the pressure is low enough. The other consideration of gas pressure is that there ought to be enough in the chamber to produce a sufficient number of ions. It has been found experimentally that 5×10^{-5} torr [8] is sufficient for both considerations, see Figure 8.

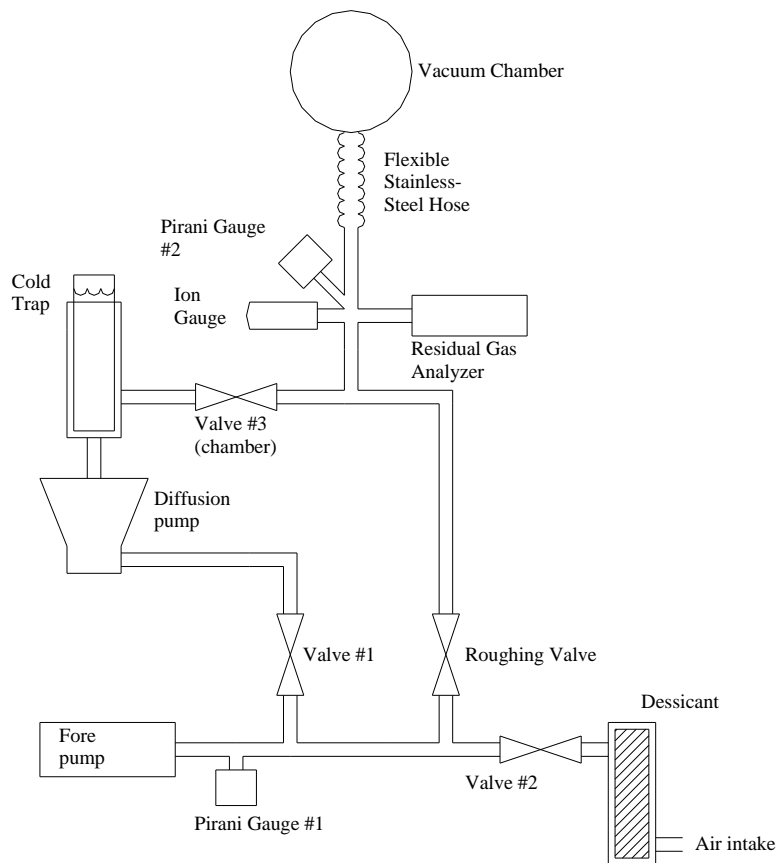


Figure 14. A schematic of the vacuum system. The fore-line pressure is measured with pirani gauge #1 and the pressure closer to the chamber with pirani gauge #2 and an ion gauge. After the system is pumped down to 10^{-3} torr the roughing valve is closed, liquid nitrogen is added to the cold trap, and the diffusion pump is turned on. These then reduce the pressure to about 5×10^{-6} torr. When the system is shut down, air is allowed into the system through the dessicant to reduce water vapor levels in the system.

The diffusion pump consists of two sections, the lower reservoir and the upper gas trap. In the reservoir Dow Corning 704 Diffusion Pump Fluid silicon oil is heated by an electrical heating element at 120 VAC, drawing about .5 A, and is released in the upper portion of the pump by jets which direct the oil downwards and outwards. The oil collides with gas molecules and moves them down and to the walls of the pump, which is chilled by a water-cooled copper tube wrapped around the outside of the wall. The oil is thickened by the lower temperature and carries the gas downwards towards the exhaust, where it can be removed by the fore-pump. The oil is then reheated and reused.

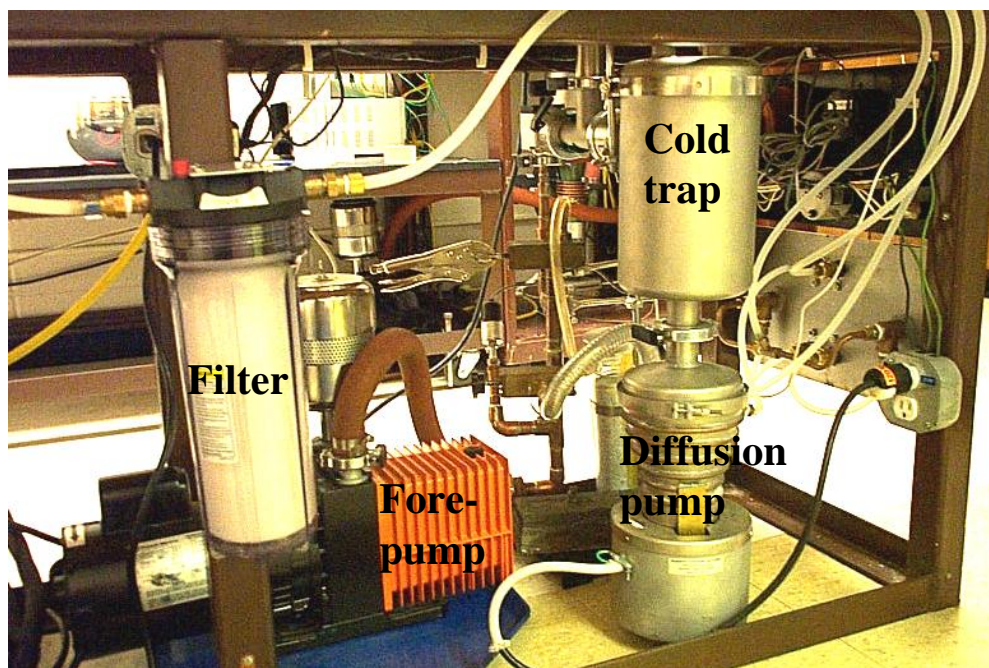


Figure 15. A photograph of vacuum pumps. Clearly visible is the Kurt J. Lesker TNR6XA150QF cold trap, Innovac R220 diffusion pump, and the CIT-ALCATEL 2012A rotary fore-pump. The water filter for the cooling system is also visible.

The cold trap is placed directly above the diffusion pump in order for it to act both as a baffle to contamination from backstreaming diffusion pump oils, and also so that chilled gas molecules that did not freeze to the cold trap are more likely to be removed by the diffusion pump, as they fall into it due to gravity. It consists of a liquid nitrogen reservoir set into a chamber that is part of the vacuum system.

Three gauges and a residual gas analyzer were used to analyze the vacuum in the chamber. A KJL-6000 0904B thermocouple, or pirani gauge #1, is read out on an analog meter and is used to monitor the fore-line pressure. Pirani gauge #2, a Granville Phillips Convectron CVT-275-101, is mounted

closer to the chamber and is used to establish the points at which to activate the diffusion pump and cold trap. Thermocouples use a coil of wire set in the vacuum and the fact resistance of the wire is proportional to its temperature to determine the pressure. Each collision with gas molecules removes some of the heat from the wire, lowering the measured resistance, and the higher the pressure, the more gas, the more collisions, and the lower the resistance.

A Duniway 1-100-K Granville Phillips 275006 ion gauge is mounted near the second Pirani gauge to measure high vacuum levels. The ion gauge consists of three main parts, the filament, the grid, and the collector. The filament is heated with an electric current that causes it to emit electrons. Some of these electrons are emitted towards the positively biased grid, and pass through. Repulsed by the negatively biased collector that is inside the grid (or coil) some of these electrons collide with gas molecules in the chamber, and ionize them. These new positive ions are attracted to the collector, and provide an electrical current that can be translated into a measurement of the gas density, and hence the pressure. Before the cyclotron is tested, the ion gauge will be mounted directly off the vacuum chamber to allow a measurement of the vacuum where the ions will be accelerated.

The residual gas analyzer, an SRS RGA 100, is used to determine total pressure in the system and the partial pressure of residual gases. The actual operating pressures will be monitored using the ion gauge and RGA, since thermocouples are only reliable at pressures above about 10^{-3} torr. The main components of the RGA are the ionizer, the ion filter, and the detector, shown in Figure 16.

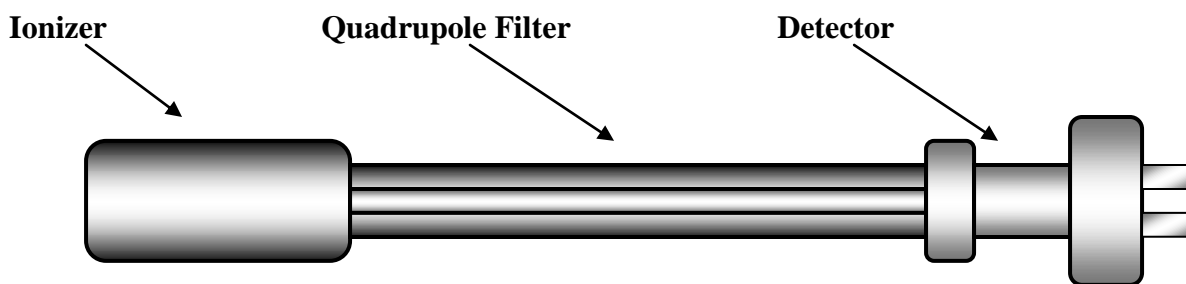


Figure 16. A schematic of the SRS RGA 100. The device consists of the ionizer, the quadrupole filter, and the detector. Electrons emitted in the ionizer ionize the local gas, which then travel into the filter. There the desired mass/charge ratios can be selected to reach the detector.

The ionizer consists of a cylindrical anode grid in the center which passes through a circular thoriated iridium filament, with both sheathed by the negatively charged cylindrical repeller. Electrons emitted

by the filament are attracted centrally towards to the anode, and most pass right through both walls of the grid, entering and exiting the region of space bounded by the anode. Upon exiting the far side of the anode they are repelled by the repeller on the other side. They change direction pass through the anode grid again. In this fashion the emitted electrons have many passes through the ionizer to increase the level of ionization. Ions leave via one end of the cylinder, repulsed by the anode when they are close enough to the open end. After passing through the aperture in the focus plate the ions enter the quadrupole ion filter. The filter, shown in Figure 17, consists of four cylindrical parallel electrodes placed at the four corners of a square.

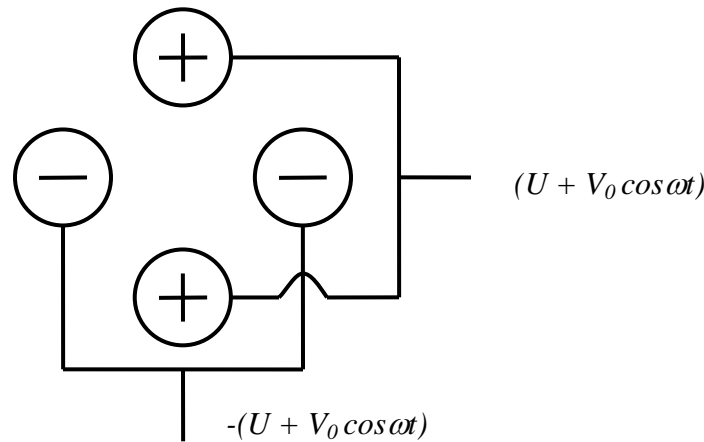


Figure 17. Schematic of RGA quadrupole filter. By selecting specific values for U and V_0 all ions without the proper mass/charge ratio are unable to navigate the length of the filter. By changing the voltages other ions can be selected for.

Electrodes lying on the same diagonal are electrically linked to an oscillating voltage source, one pair is linked to a voltage of $U + V_0 \cos \omega t$ and the other pair to a voltage of $-(U + V_0 \cos \omega t)$, where U is some DC voltage, V_0 is some AC voltage, ω is the angular frequency, and t is time. The ions from the ionizer travel down the length of the filter between the four electrodes, and due to the oscillating voltages on these electrodes the ion trajectories wobble. Most ions do not successfully travel the length of the filter and never make it to the detector. By selecting values of U and V_0 the filter removes all but one mass/charge ratio out of trajectory, which can then be detected. By changing the values of the DC and AC voltage, different mass/charge ratios can be selected.

The vacuum system has been tested using the residual gas analyzer, the results of which are shown in Figure 18.

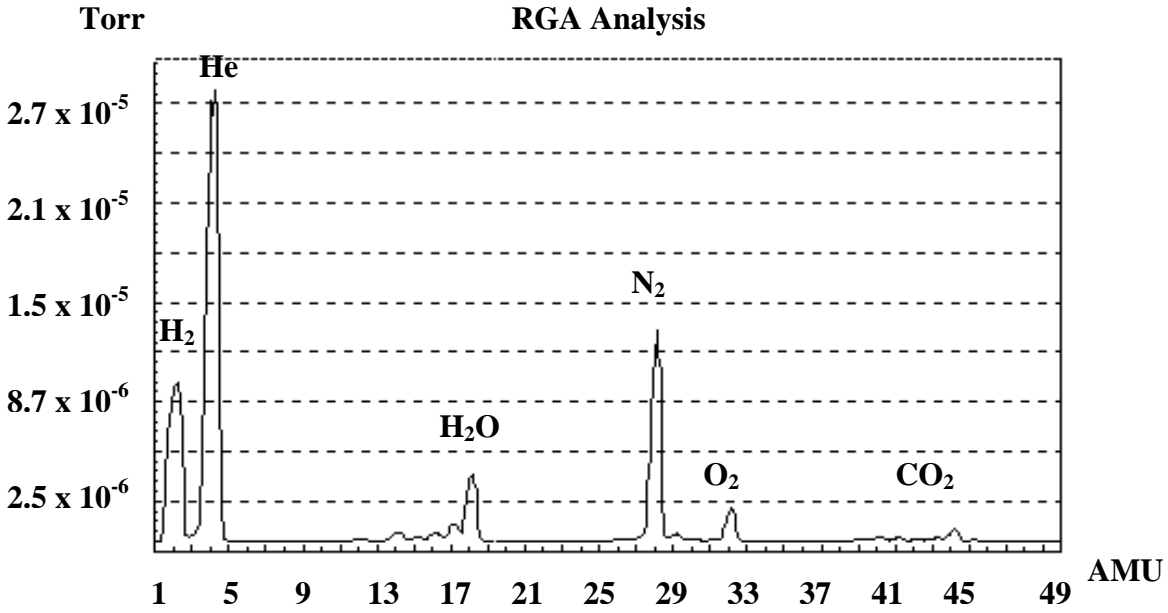


Figure 18. A plot of the RGA analysis. Helium was allowed into the chamber, all other peaks but the hydrogen are due to gases from the atmosphere. The presence of such a large concentration of hydrogen is still unexplained.

The first peak is due to molecules of hydrogen, which is outgassed by the stainless steel components of the vacuum system. The second peak is helium which was allowed into the system through a needle valve. The rest of the peaks are water vapor, nitrogen, oxygen, and carbon dioxide, which are atmospheric gases.

3.3 The Cooling system

Both the electromagnet and the diffusion pump require a chilled water system for cooling, shown in Figure 19. The water chiller used is a Haskris model ASH type A with a maximum output of about 3.8 L per minute at 20° C. It supplies 0.75 L per minute to the diffusion pump and 3 L per minute to the electromagnet through 0.95 diameter polyflow tubes. The supply line is split in the accelerator room, and each of the two branches is controlled by a different valve. Both lines run to their respective flowmeters, and from there one goes to the diffusion pump and the other to the magnet. If the magnet is not supplied with 2.5 liters of chilled water per minute the interlock controls will power down the magnet. After running to the diffusion pump and magnet, the water return lines are then reconnected and sent back to the return on the chiller.

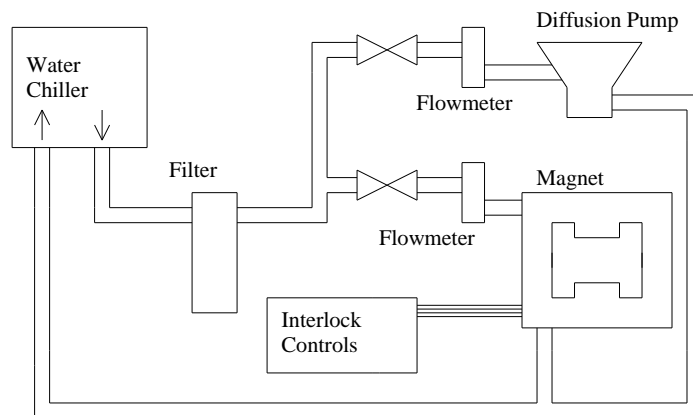


Figure 19. A schematic of the cooling system. Chilled water runs from the chiller to the apparatus, where the line splits into two separate lines. Both are controlled by separate valves and adjusted and monitored with flowmeters. The two lines supply the diffusion pump and electromagnet with chilled water and then return to the chiller. If the magnet is not supplied with 2.5 liters of chilled water per minute, the magnet will power down.

3.4 The Electromagnet

The magnet, shown in Figure 20, is a GMW model 3473-70 with 15.2 cm pole faces and an adjustable pole gap of 0 to 9.9 cm.

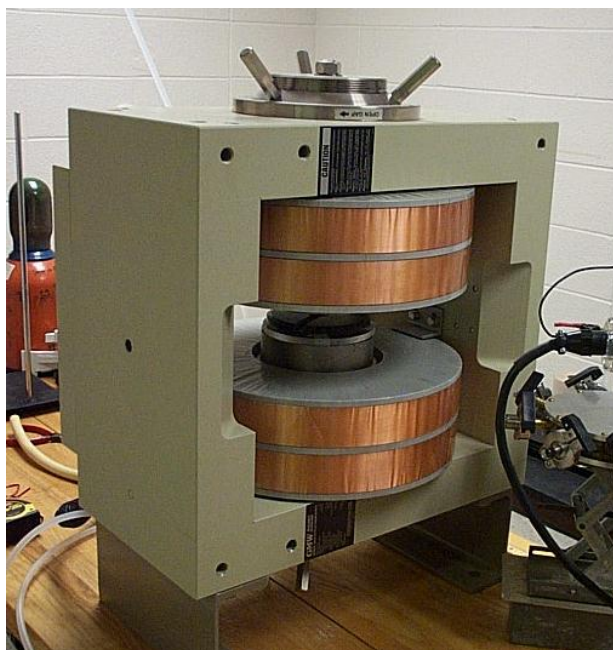


Figure 20. A photograph of the GMW 3473-70 electromagnet. It has 15.2 cm pole faces, an adjustable pole gap of 0 to 9.9 cm, and can draw up to 70 A.

The maximum current useable with the magnet is 70 A and at that current the magnet consumes 4.1 kW of power. The power supply however, a Powerten R62B-4050, can only support a maximum of 50 A, at which the magnetic field strength is 1.127 T. At maximum current the magnet requires 6 liters per minute of water at 20° C to cool the coils, but at 50 A only requires 3 liters per minute. The magnetic has a mass of 610 kg and measures 68.6 cm wide by 40.5 cm deep by 57.0 cm tall. There is an interlock which shuts down the magnetic if less than 2.5 liters per minute of chilled water are supplied, or if the temperature of any one of the coils exceeds 50° C. In the future, a more powerful chiller and power supply may be acquired which would allow using the magnet at the maximum current of 70 A.

The magnetic field was measured with the magnet pole faces set to a 3.9 cm gap, because this is the pole gap required to accept the vacuum chamber. It was assumed that the magnetic field strength at all points would scale linearly with the magnetic field at the center. Based on this assumption, the magnetic field at the center of the pole faces was measured as a function of current supplied to the magnet, which combined with a map of the field can be used to determine the field strength anywhere for a given current. Figure 21 is the result of this measurement, in blue triangles, and a plot of the same information supplied by the manufacturer, in red squares.

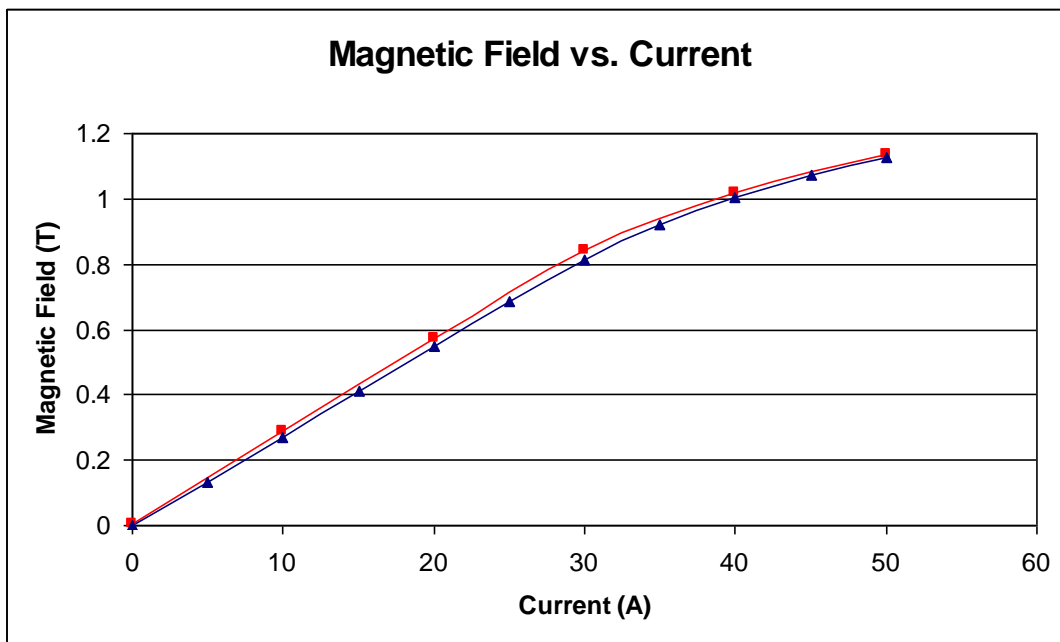


Figure 21. A plot showing how the magnetic field strength increases as a function of current supplied to the electromagnet, as measured at Houghton (blue triangles) and by the manufacturer (red squares). The measurements were taken at the center of the region of space between the two pole faces.

The field was mapped using an acrylic disc, an aluminum disc that was marked with the 360 degrees of a circle, and a F. W. Bell 5070 Teslameter. The acrylic disc was milled to fit the aluminum disc such that they shared the same axis of symmetry, and so that the aluminum disc could rotate freely. The acrylic disc was attached to the lower pole face with tape, and the aluminum disc was set into the milled groove. The aluminum disc was milled to hold the Teslameter so that the probe could slide radially. Tape held the Teslameter in place for each measurement. Figure 22 is a plot of the magnetic field versus the radius at 25 A as measured by Houghton in blue triangles, and by the manufacturer in red squares. The pole faces have a radius of 7.62 cm.

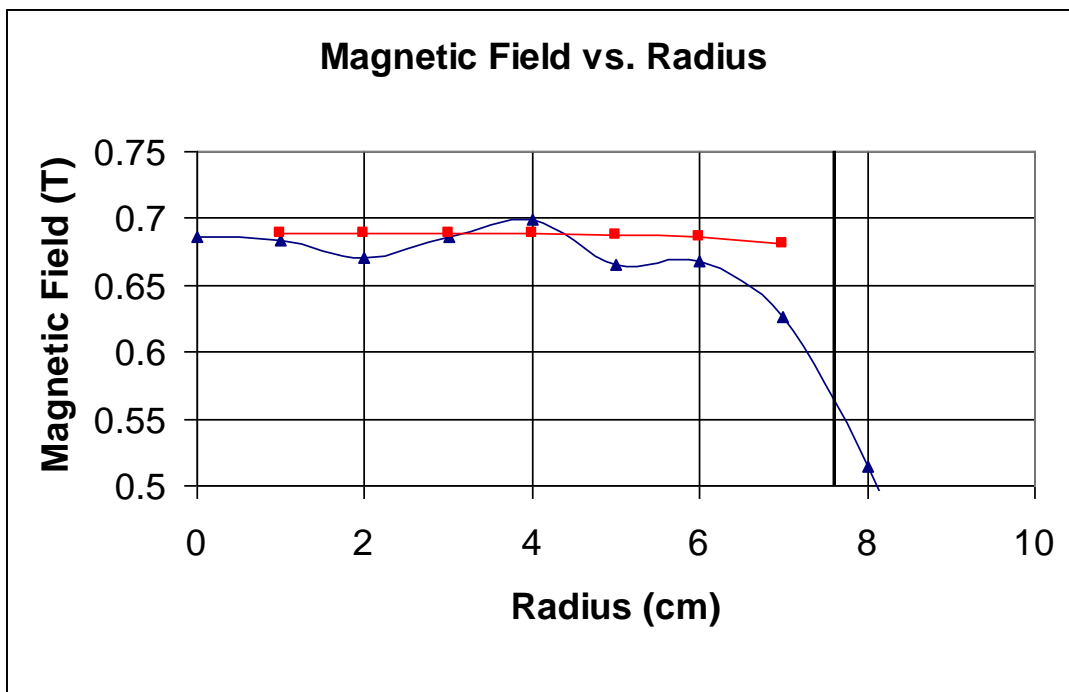


Figure 22 A plot of the magnetic field of the magnet at 25 A by Houghton in blue triangles and by the manufacturer in red squares. The pole faces of the magnet have a radius of 7.62 cm.

The Houghton results do not agree well with information provided by the manufacturer. However, because of the flaws in the Houghton College mapping apparatus and the probable misuse thereof, it is quite possible that the magnetic field is more closely represented by the manufacturer's results. It is also interesting to plot the index of this magnet, as seen in Figure 23. It is what was expected, a value of zero in the center to much higher values in the fringe field.

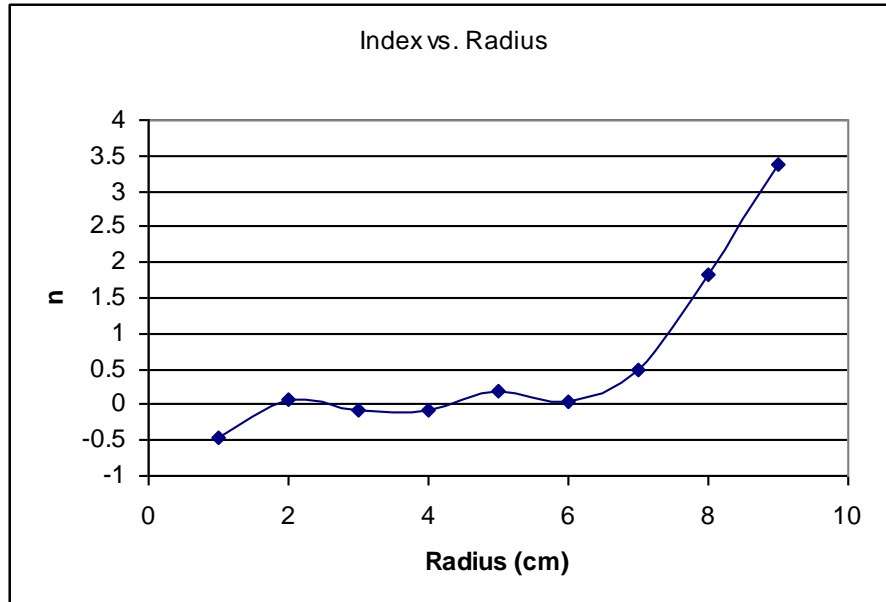


Figure 23. A plot of the index of the magnet. It ranges from zero in the center of the magnet to almost 3.5 in the fringe field. The most desirable shape to this curve is a linear increase, but the index can be changed by shaping the field with ferromagnetic shims.

This is a far cry from the linear increase of n that is most desirable for resonance and focusing reasons, however, it should be possible to shape the field using ferromagnetic shims. Also, data from the manufacturer does not extend into the fringe field, so the index over the given range, 0.5 cm to 5 cm, is nearly a constant zero.

3.5 The Chamber

The main components of the chamber are the vacuum chamber, shown in Figure 24, the electrodes in the chamber, shown in Figure 26 and the ion source, also shown in Figure 26.

3.5.1 The Vacuum Chamber

The vacuum chamber, drawn in Figure 24 and photographed in Figures 25 and 26, consists of a .9 mm thick by 2.5 cm wide strip of brass soldered to the inside of two 0.6 cm by 0.6 cm rings of brass, with inner diameter 15.2 cm and separated by 1.3 cm. Eight 1.3 cm diameter holes are drilled into the brass strip at intervals of 45° to accommodate the eight quick flanges that are soldered in each hole. The top and bottom plates are 0.64 cm thick type 6061T6 aluminum 17.1 cm in diameter with eight holes drilled for 8-32 brass screws which are used to hold the chamber together. The top plate has holes large enough for the screws to slide through, and holes in the bottom plate are tapped so that the plates screw together, sandwiching the brass ring in between. Each plate is milled with a 3.28 cm wide

by 0.25 cm deep groove with an inner diameter of 15.24 cm to accommodate a 0.32 cm thick Viton O-ring. The top chamber is also milled to have a shallower section in the center to accommodate the filament, which is higher than the other elements in the chamber, and so needed more space to avoid shorting with the plate.

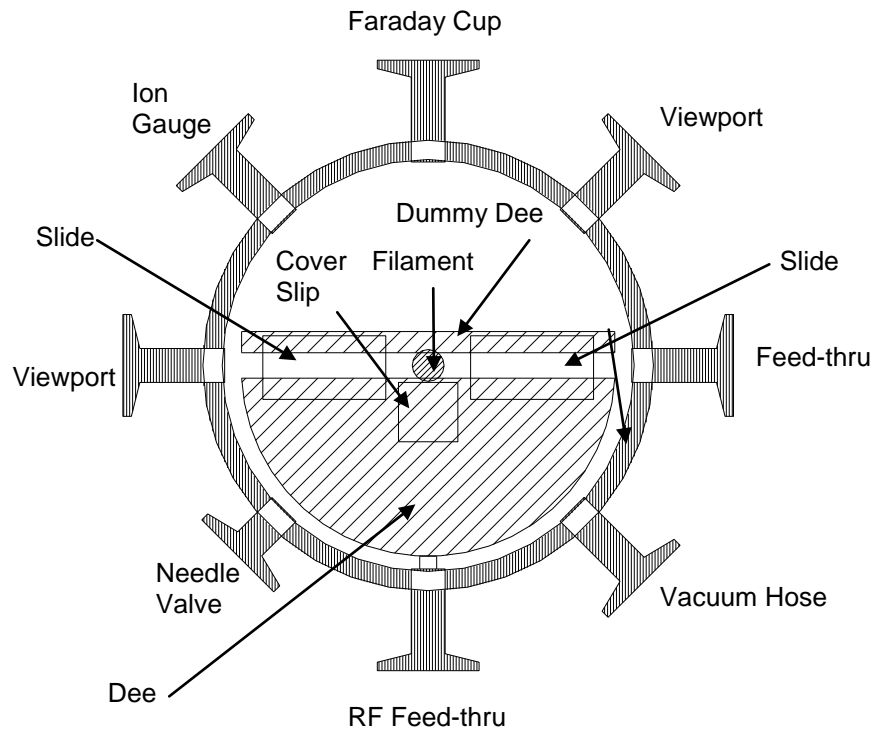


Figure 24. A drawing of vacuum chamber. The brass ring is drilled with eight holes allowing the brass quick-flanges to be soldered in. The copper dee is connected to the RF source via a feed-thru, and is connected to the dummy dee with epoxy and glass microscope slides. The dummy dee is held at ground through the feed-thru on the right, which also is used to connect the filament to the power supplies. The cover slip is to provide insulation, as connectors for the filament wires are glued on top of it.

The eight ports are used for two QF16-075-VP Kurt J. Lesker glass viewports, one Kurt J. Lesker EFT1213258 power feed-through for the dee, one multiple Kurt J. Lesker EFT0082038 feed-through for the filament and grounding the dummy dee, one for the faraday collector, one for releasing gas into the chamber, one to connect to the ion gauge, and one to connect the chamber with the vacuum pumps.



Figure 25. A photograph of the vacuum chamber situated between the magnet pole faces. The ring is made of a strip of brass and two outer rings to which the strip is soldered, and eight quick flanges that are soldered in place around the ring. Two aluminum plates equipped with O-rings are screwed together around the ring to form a vacuum tight seal. The device is centered between the pole faces of the magnet.

3.5.2 *The Electrodes*

The dee electrode consists of two equally sized semicircular plates of 0.9 mm thick copper which were cut from a circular sheet with a diameter of 145 mm. A strip of copper of the same thickness was cut, 1.57 mm wide, and then soldered to the other two pieces to form a semi-circular hollow electrode, shown in Figure 26. The open face of the dee was squared using a milling machine, to give the final dimensions of 14.3 mm thick, 142.4 mm from front to back and 68 mm from side to side. A hole is drilled in the back side of the dee to allow an 8-32 brass screw to hold it to the feed-through. A locking washer was used to keep the screw from loosening and the dee from spinning. The dummy dee is made from two 0.9 mm thick by 5 mm wide strips of copper, one 171.5 mm long and the other 142.9 mm long. The longer piece was bent to form three sides of the rectangular electrode and the shorter piece was placed on top. Also, a small piece of MDC Vacuum Products KAP2 copper wire is soldered to the top piece, which then connects with a wire from the feed-through through a barrel connector so that the dummy dee can be grounded.

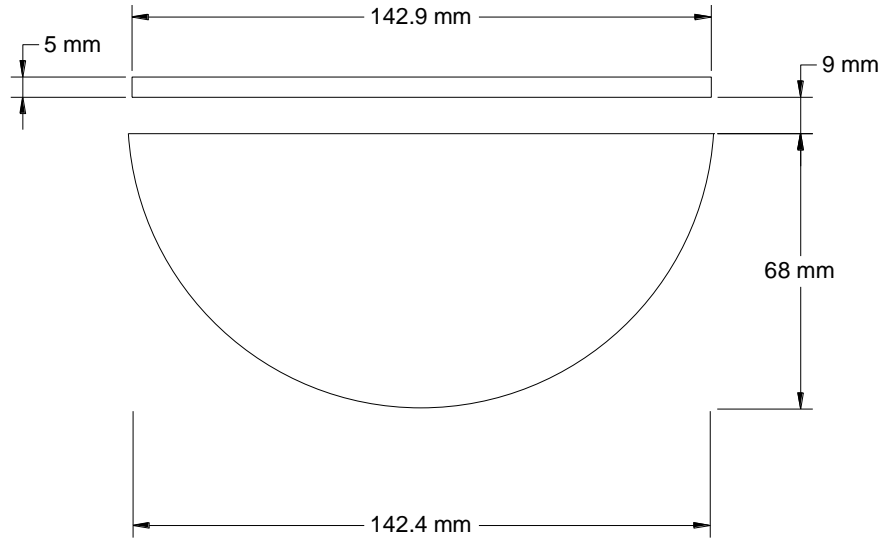


Figure 26. A top view drawing of the electrodes with dimensions labeled.

The two electrodes were held together by three insulating glass microscope slides, which were glued to the copper with Loctite 1C Hysol vacuum epoxy, as can be seen in Figure 27.



Figure 27. A photograph of the electrode assembly. The copper dee is held to the dummy dee with three glass microscope slides glued in place with vacuum epoxy. The grounding wire can be seen on the dee, as well as the feed-throughs. The filament is held in place with short wires soldered to the contacts and barrel connectors, held to the dee with epoxy and insulated by a microscope cover slip.

3.5.3 The Ion Source

The gas used to produce ions will be allowed into the chamber via an Edwards LV10K needle valve. Some of these gas molecules will be ionized by a filament from an AET EM6G electron microscope. A potential across the filament of 1.5 V, results in a current of 2.3 A and the filament floats at least 100 V above ground to produce energetic electrons capable of ionizing the gas. It was found that even with the maximum magnetic field the filament was strong enough to effectively resist the Lorentz force upon the filament. The positive ions will then be accelerated by the cyclotron, and the electrons, being much lighter, will travel in tight helices vertically downward to the bottom of the chamber. The filament is held in place between the two electrodes by two short copper wires which were soldered to the filament contacts. These wires are in turn held by metal barrel connectors that were epoxied to a microscope cover slip insulator which was glued to the dee. The barrel connectors can be connected to the wires from the feed-through to energize the filament.

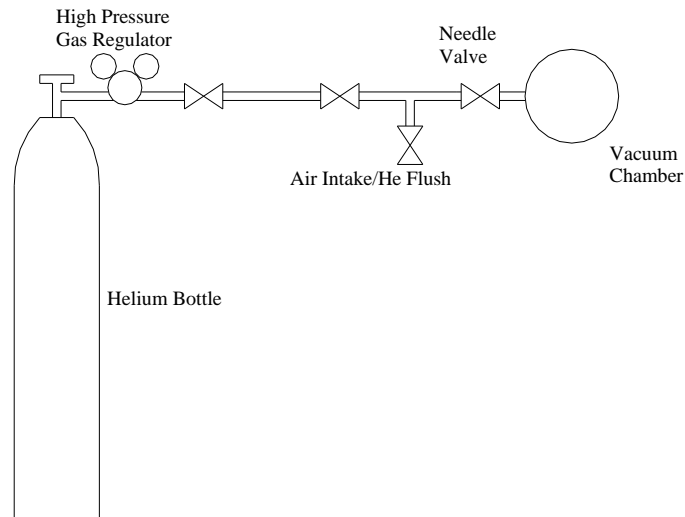


Figure 28. Schematic of the gas handling system. The air intake valve/He flush valve is used to flush undesirable gases from the line and to let air back into the system.

The gas handling system, Figure 28, is also a part of the ion source. It consists of a high pressure gas cylinder, a high pressure gas regulator, 0.64 cm copper tubing, a series of valves, and the Edwards LV10K needle valve attached directly to the vacuum chamber with a quick flange. The system can be flushed with the gas from the cylinder by closing the needle valve and opening the helium flush valve. The higher pressure helium will force the air in the line into the atmosphere, so that it does not

contaminate the gas. By using the needle valve and the regulator control, the pressure of helium in the vacuum chamber can be controlled in the 10^{-6} to 10^{-5} torr range.

3.5.4 Faraday Collector

To obtain a measurement of the beam current, a Faraday collector has been built using the bellows and housing of a right angle brass Veeco valve, shown in Figure 29.

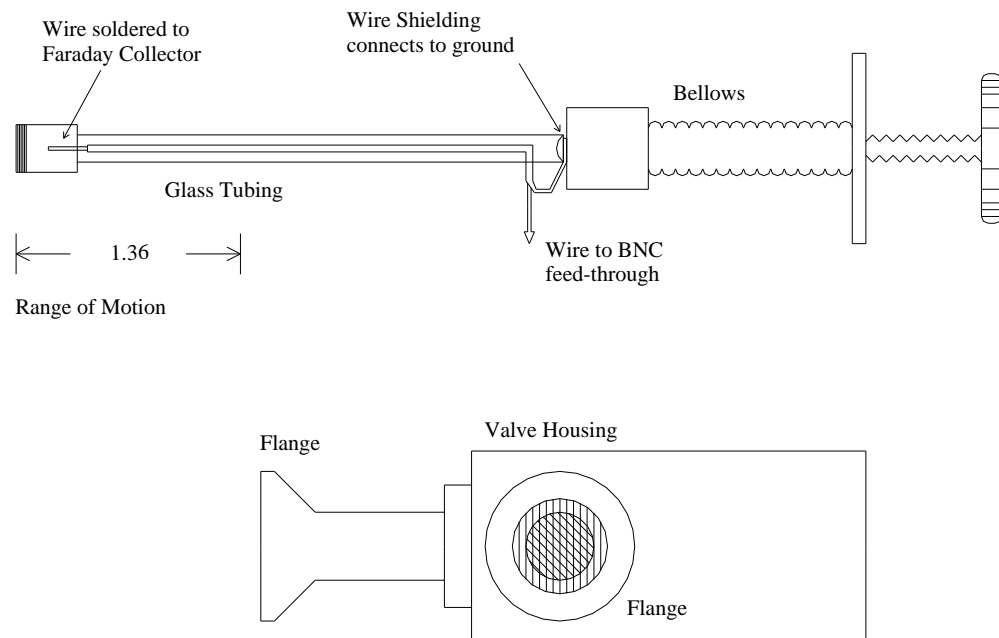


Figure 29. A schematic of the Faraday collector assembly. The long glass tube insulates the collector from ground, while the wire used is shielded coaxial cable to prevent RF voltage from interfering with the current reading. The collector itself is a small copper box with aluminum foil top. It can be moved into and out of the chamber 1.36 cm by use of the valve bellows.

The bellows can be moved 1.4 cm in and out, allowing to measurement of the beam current in the chamber at various radii. A small brass screw was bored through its axis to allow air to escape the screw hole, and is screwed into the end of the bellows. On this screw was glued a 9.7 cm length of 5.5 mm diameter glass tubing with a small hole drilled in its side near the bellows end. Through this hole was threaded a shielded MDC Vacuum Products KAP3 high vacuum coaxial cable that carried the signal from the faraday collector glued to the end of the glass tube. The wire is connected to a BNC feed-through with a barrel connector, and the shielding is twisted off and secured to the bellows, which are at ground potential, by the brass screw that supports the glass rod. The faraday

collector consisted of a small copper box to collect the ion current, approximately 7.5 mm wide by 8.5 mm long. The top of the box slopes down, from 7.0 mm to 5.0 mm towards the glass rod from the front to back in order to discourage particles from bouncing directly out of the collector. The box has a slit about 1.5 mm wide running across the end of the face that would be turned towards the positive ion current. The end of the box was constructed of aluminum foil, chosen because it was thin so as not to block the revolving ions before they could enter the cup itself. The current will be measured by an Hewlett Packard 617 Electrometer.

3.6 Radio Frequency Circuit

As of the writing of this thesis, the RF circuit has not been constructed. It is planned to use a coaxial mutual induction circuit to couple the chamber to the output of an ENI 155LCRH RF Power Amplifier. The primary coil for the transmatch will be the outer coil and directly connected to the amplifier. The secondary coil will be electrically connected to the feed-through from the dee. It should be noted that all elements in the oscillating circuit need to be shielded to prevent the resultant radiofrequency waves from disrupting other devices which use a similar frequency as the cyclotron.

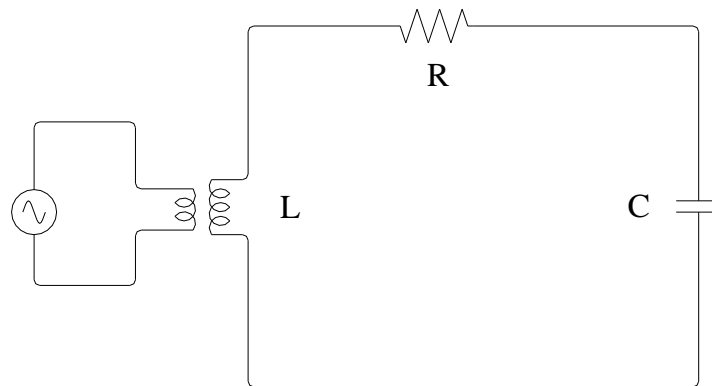


Figure 22. A schematic of the circuit used to drive the dee. The circuit includes a capacitor which is composed of the dee and chamber, some inherent resistance in the system, and the inductor which is part of the transmatch. The transmatch uses induction to link the dee to the driving circuit.

The planned oscillating circuit is a driven RLC circuit, shown in Figure 30. The inductance in the circuit is a result of the transmatch system which is simply a core-less transformer, making use of mutual inductance. The capacitance in the circuit is provided by the dee and vacuum chamber: as a large conducting plate to which a voltage is applied, it acts as a capacitor. In driven RLC circuit it is

possible to achieve resonance, if the capacitance and inductance are carefully chosen. The impedance of the circuit, Z , is expressed as

$$Z = \sqrt{R + (X_L - X_C)^2}, \quad (20)$$

where X_L is the reactance due to the inductor, X_C is the reactance contribution from the capacitor, and R is the resistance of the circuit. When $X_L = X_C$ the impedance of the circuit is at its lowest value, dependent only on the resistance, and the circuit is at resonance which means the current and voltage are at their maximum values. However, both inductive and capacitive reactance depends on the frequency of oscillation, f :

$$X_L = 2\pi fL \quad (21)$$

$$X_C = \frac{1}{2\pi fC} \quad (22)$$

where L is the inductance and C is the capacitance. Thus, the frequency of oscillation and therefore the strength of the magnetic field must be chosen before the circuit can be constructed. Once the frequency is known, the inductance can be chosen to fit the resonance condition:

$$f_0 = \frac{1}{2\pi\sqrt{LC}}, \quad (23)$$

where f_0 is the resonant frequency. The level of resonance achieved will determine the peak voltage difference between the grounded elements of the cyclotron and the dee. In order to avoid sparking in the gaps in the cyclotron chamber, the voltage supplied by the amplifier must be carefully chosen. The peak voltage across the capacitor is given by

$$V_{C,peak} = I_{peak} X_C = \frac{I_{peak} 2\pi}{Cf}. \quad (24)$$

The quality of a resonance is measured by how sharp of a peak it is, which is given by the “Q” value. The Q value is defined as the resonance frequency divided by the bandwidth, or the frequency range

of the peak. So, the wider the peak the peak is the greater the bandwidth will be, and so it corresponds to a lower quality factor. The bandwidth, Δf is related to the damping factor ζ , given by

$$\zeta = \frac{R}{2L}, \quad (25)$$

by the following equation,

$$\Delta f = \frac{\zeta}{\pi}. \quad (26)$$

So the quality factor Q is given by

$$Q = \frac{1}{R} \sqrt{\frac{L}{C}}. \quad (27)$$

Since no resistance is being added to circuit, a relatively high Q value is expected. Also, it has not been determined how high the voltage ought to be for the Houghton College cyclotron, but once a figure is arrived at (24) will be used to determine the current supplied by the RF power amplifier.

The capacitance of the dee and chamber of the Houghton College cyclotron has been determined to be 79 pf. If the maximum magnetic field of 1.127 T is used then the frequency of orbit for singly ionized helium is 4.32 MHz, and thus the inductance, using (23), must be 17.2 μ H. In this system the maximum energy for singly ionized helium is 77.2 keV. For doubly ionized helium, the frequency in the same magnetic field is 8.63 MHz, so the inductance is 4.29 μ H, and the maximum energy is 309 keV.

3.7 Electronics

The control electronics of the experiment, shown in Figure 31, are connected to a National Instrument GPIB-enet converter via a General Purpose Interface Bus. The converter allows a computer running Labview 7.0 to control the cyclotron remotely via an Ethernet network.

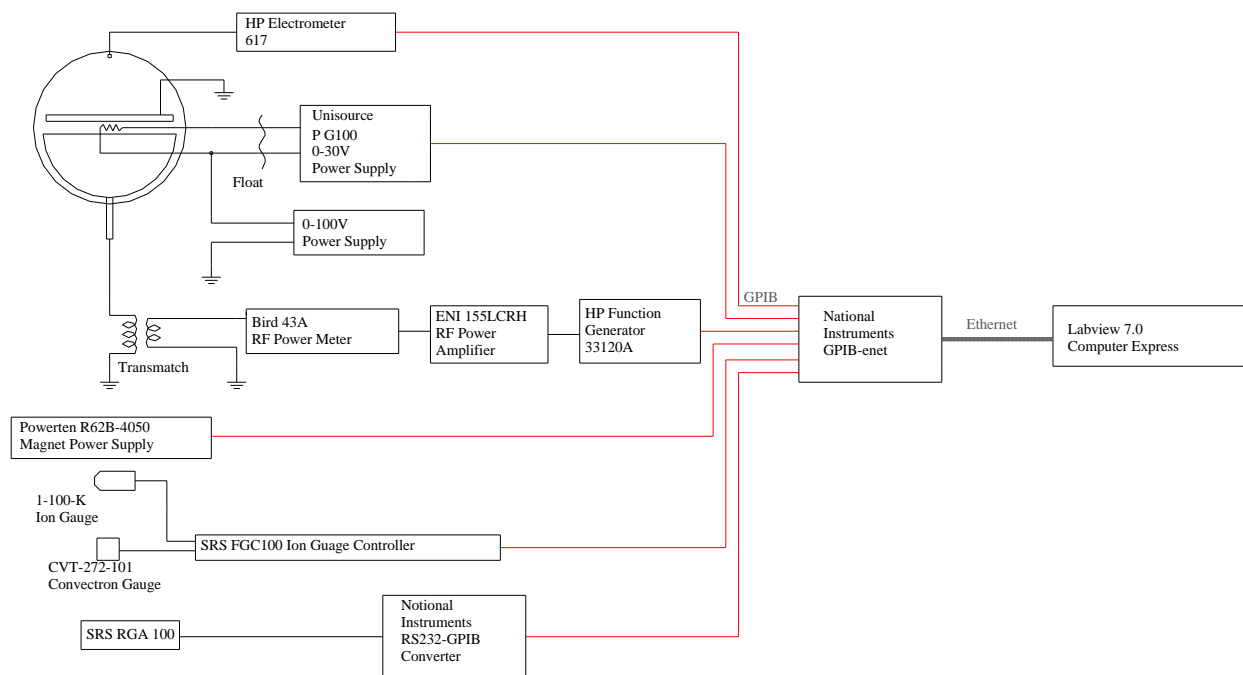


Figure 31. An electronics diagram. All of the electronics, with the exception of the floating filament power supply, are monitored and controlled remotely through the general purpose interface bus. The National Instruments GPIB-enet allows these instruments to be controlled through an Ethernet network.

The 1-100-K Ion gauge and CVT-272-101 Convecatron gauge are connected to an SRS FGC 100 Ion Gauge Controller, where they measurements can be displayed, converted to GPIB, and relayed to the GPIB to Ethernet converter. The SRS RGA 100 connection is RS232, and so it needs the National Instruments RS232-GPIB Converter to connect it to the bus. The Powerten R62B-4050 magnet power supply supports a GPIB connection and needs no converter. The power in the primary coil of the transmatch is monitored by a Bird 43A RF power meter, and supplied by the ENI 155LCRH RF power amplifier. The RF signal is provided by the HP 33120A function generator which connects to the GPIB. The filament in the chamber is powered by an Unisource PG100 0-30V power supply which is controlled through the bus. The voltage on the filament floats on the voltage provided by 0-100V power supply to provide the emitted electrons a higher energy to increase the ionization rate. Finally, the Faraday collector signal is read by an HP 617 electrometer which is directly connected to the GPIB bus.

Chapter 4.

Conclusion

4.1 Summary

Results from the Houghton College cyclotron are expected soon. The vacuum system has been tested and can maintain a vacuum on the order of 10^{-6} torr, and the pressure of introduced gas in the vacuum system can be controlled with the gas handling system. The filament has been tested in the chamber up to about 2.5 A. The cooling system has been built and tested. The magnetic field has been mapped and shown to have a maximum field of 1.127 T. The Faraday collector has been built and needs to be tested, and the resonating circuit needs to be tuned and tested.

4.2 Future Plans

The immediate plan for the future is to complete and test the cyclotron. Longer range plans include building a larger vacuum chamber and electrodes that would allow full advantage to be taken of the diameter of the magnetic field. Also, the magnetic field could be shimmed with ferromagnetic materials, thereby adjusting the shape and strength of the field. Once the cyclotron meets certain operational and consistency standards, it is planned to use it for producing neutrons. This will be accomplished with a deuteron-deuteron reaction, $d(d,n)^3\text{He}$. Deuterium gas will replace the current helium gas, and the deuterium nuclei will be ionized and accelerated. A copper target will be placed in the chamber, which will as a result of the beam be impregnated with deuterons. More ions from the beam will collide with the trapped deuterons, undergoing one of two reactions, $d(d,n)^3\text{He}$ or $d(d,p)^3\text{H}$. Since neutrons are the desirable result of the reaction, no extraction system will be required. The protons produced by the $d(d,p)^3\text{H}$ reaction will likely be stopped by the vacuum chamber walls, while the neutrons will simply pass unhindered through the interposing materials. These reactions are exothermic with 2.227 MeV released for each deuteron pair. Figure 32 is a plot of the cross section of the reaction against deuteron energy.

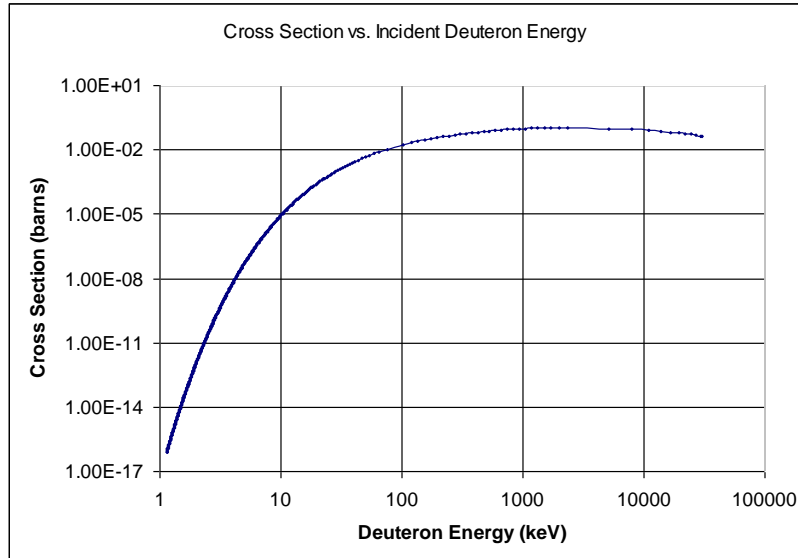


Figure 32. Plot showing the cross section, which is a measurement of the probability for the reaction to occur, of the $d(d,n)^3\text{He}$ reaction as a function of incident deuteron energy. The maximum energy of the Houghton College cyclotron is expected to be 150 keV.

Cross section is a measurement of the probability for the reaction to occur, so the higher the cross section of the reaction the more neutrons are produced; this is the primary reason to increase the maximum energy of the Houghton College Cyclotron. All the machine must provide is enough energy to overcome the Coulomb repulsion of the deuterons, so that the desired reaction can take place. The maximum energy of the current cyclotron, using (6), is 150 keV for deuterons, which puts the cross section near the maximum. With this incident deuteron energy and the exothermic properties of the reaction, the maximum energy for neutrons by the Houghton College cyclotron will be approximately 2.8 MeV.

References

- [1] H. W. Geiger and E. Marsden, *Proc. Roy. Soc.* **82**, 495 (1909).
- [2] H. Geiger and E. Marsden, *Philos. Mag.* **27**, 604 (1913).
- [3] J.D. Cockroft and E.T.S Walton, *Proc. R.Soc. London* **A136**, 619 (1932); **A137**, 229 (1932).
- [4] R. J. Van de Graaff, K. T. Compton, and L. C. Van Atta, *Phys. Rev.* **43**, 149 (1933).
- [5] R.J. Van de Graaff, *Proc. Amer. Phys. Soc. Meeting*, Sept 10, 11, 12, 1931.
- [6] M. S. Livingston and J. P. Blewett *Particle Accelerators* (McGraw-Hill Book Company, 1962)
- [7] R. Wideröe, *Archiv für Electrotechnik* **21**, 387 (1928).
- [8] D. H. Sloan and E. O. Lawrence, *Phys. Rev.* **38**, 2021 (1931).
- [9] E. O. Lawrence “The Evolution of the Cyclotron.” Nobel Lecture, December 11, 1951.
- [10] M. S. Livingston, Ph. D. Thesis, University of California. 1931.
- [11] E. O. Lawrence and M. S. Livingston, *Phys. Rev.* **40**, 19 (1932).
- [12] E. O. Lawrence, M. S. Livingston, and M. G. White, *Phys. Rev.* **42**, 150 (1932).
- [13] H. A. Bethe and M. E. Rose, *Phys. Rev.* **52**, 1254 (1937).
- [14] CERN Annual Report 2004, 2005).
- [15] A. G. Ingalls. *Sci. Am.* **189.3**, 154 (1953).
- [16] B. V. Siegel and R. C. Sinnott, *Phys. Today* **1**, 10 (1948).
- [17] J. J. Welch, K.J. Bertsche, P.G. Friedman, D. E. Morris, and R. A. Muller, *Advanced Accelerator Methods: The Cyclotron*. 1987.
- [18] Fred Niell, *Cyclotron Notes*. 2002.
- [19] “Rutgers Cyclotron” <http://www.physics.rutgers.edu/~koeth/cyclotron/> (Viewed **February 23**, 2006).
- [20] Toni Feder, *Phys. Today* **57**, 30 (2004).
- [21] Jeffrey C. Smith, Undergraduate Thesis, Knox College, 2001.
- [22] M. E. Rose, *Phys. Rev.* **53**, 392 (1938).